PHARMACOSYNTHETIC MODULATION OF SEROTONIN NETWORKS

Daniel Jason Urban

A dissertation submitted to the faculty of the University of North Carolina at Chapel Hill in partial fulfillment of the requirements for the degree of Doctor of Philosophy in the Department of Pharmacology

Chapel Hill
2013

Approved by:

Ken McCarthy

Bryan Roth

Thomas Kash

Robert Nicholas

Marc Caron

ABSTRACT

Daniel Jason Urban: Pharmacosynthetic Modulation of Serotonin Networks
(Under the direction of Bryan Roth)

Dr. Francis Crick described the brain as "an exceedingly cunning combination of precision wiring and associative nets" (Crick, 1979). While this explanation is over 30 years old, it accurately describes the complexity of the central nervous system modern neuroscientists are challenged with unraveling. The serotonergic network is an example of this intricate design. It originates from a small number of neurons relatively clustered together, but distributes its projections extensively throughout the entire CNS such that virtually every cell in the brain is in close proximity to a serotonin fiber. Advances using small molecules that augment serotonin concentrations such as serotonin selective reuptake inhibitors (SSRIs) have contributed immensely in constructing the frame work of the serotonin network and characterizing its influence on mammalian physiology and behaviors. Even so, these small molecule approaches are limited due to the global impact they have on serotonergic neurotransmission, making the neuronal mechanisms responsible for their effects difficult to discern. One approach to unraveling the complexity of the serotonin network is to dissect the system into its parts by selectively and reversibly controlling specific serotonin nuclei. In fact, Dr. Crick predicted the need for this approach stating that, "to understand a complex biological system one must be able to interfere with it both precisely and delicately at all levels, but especially at the cellular and molecular levels"

(Crick, 1999). The recently developed chemogenetic technique termed Designer receptors exclusively activated by designer drugs (DREADDs) is ideal for selectively stimulating and inhibiting subpopulations of neurons, thereby demonstrating this delicate and precise approach for elucidating neuronal function at the cellular and molecular levels. In this work, we take advantage of this technique to selectively and remotely control the largest of the serotonergic nuclei, the dorsal raphe, and examined its effects on feeding, anxiety and antidepressant-like behaviors and in turn reveal how this nucleus contributes to the wide ranging effects of the serotonergic system.

I dedicate this dissertation to my loving wife and my wonderful children. This would have not been possible without them.

ACKNOWLEDGEMENTS

I would like to acknowledge my mentor, Dr. Bryan Roth, who has guided me through this journey and has helped mold me into a more productive and methodical scientist. Additionally, Bryan always encouraged me to think big and expand my horizons. I would also like to thank Martilias Farrell and Kate White for their time and help discussing and working through all the pitfalls of my many projects. Furthermore, I would like to thank all the post-docs who were working in Dr. Bryan Roth's laboratory during my graduate school years. They have been valuable resources and have helped scrutinize my approaches when testing many hypothesizes.

TABLE OF CONTENTS

LIST OF TABLES

LIST OF FIGURES

LIST OF ABBREVIATIONS

μPET – micro Positron Emission Tomography

5-HIAA – 5-hydroxyindole Acetic Acid

5-HT – 5-hydroxytryptamine

5-HT1 – Serotonin 1 Receptor Family

5-HT1A – Serotonin 1A Receptor

5-HT1B – Serotonin 1B Receptor

5-HT1C – Serotonin 1C Receptor

5-HT1D – Serotonin 1D Receptor

5-HT1E – Serotonin 1E Receptor

5-HT1F – Serotonin 1F Receptor

5-HT2 – Serotonin 2 Receptor Family

5-HT2A – Serotonin 2A Receptor

5-HT2B – Serotonin 2B Receptor

5-HT2C – Serotonin 2C Receptor

5-HT3 – Serotonin 3 Receptor

5-HT4 – Serotonin 4 Receptor

5-HT5 – Serotonin 5 Receptor Family

5-HT5A – Serotonin 5A Receptor

5-HT5B – Serotonin 5B Receptor

5-HT6 – Serotonin 6 Receptor

5-HT7 – Serotonin 7 Receptor

5-HTT – Serotonin Reuptake Transporter Gene

A2A – Adenosine 2A Receptor

AAV – Adeno-Associated Virus

AAV – Adeno-Associated Virus

AC – auditory cortex

ACh – Acetylcholine

ACTH – Adrenocorticotropin Hormone

AgRP – Agouti-Related Protein

AOM – anterior olfactory nucleus (medial part)

AS – Active States

ASP – Active State Probability

AUC – Area Under The Curve

BDNF – Brain-derived Neurotrophic factor

BNST – Bed Nucleus of the Stria Terminalis

CAMKIIa – Calcium/Calmodulin-Activated Protein Kinase II Alpha

CART – Cocaine and Amphetamine Regulated Transcript

CBN – cerebellar nuclei

Cg1 – cingulate cortex

Cg2 – cingulate cortex 2

CGRP – Calcitonin gene related peptide

CNO – Clozapine-N-Oxide

CNS – Central Nervous System

Cre – Cre-recombinase enzyme

CREB – Cyclic-AMP-Response-Element-Binding Protein

CRF – Corticotropin-Releasing Factor

CSF – Cerebral Spinal Fluid

CT – central thalamic nucleus

CT – Circadian Time

D1 – Dopamine 1 Receptor

D2 – Dopamine 2 Receptor

DBS – Deep Brain Stimulation

DC – Dark Cycle

DG – dentate gyrus

DMSO – Dimethyl Sulfoxide

DOPAC – 3,4-dihydroxyphenylacetic Acid

DR – Dorsal Raphe

DRC – Dorsal Raphe Caudal

DRD – Dorsal Raphe Dorsal

DREADD – Designer Receptor Exclusively Activated by Designer Drug

DREAMM – DREADD Assisted Metabolic Mapping

DREAMM – DREADD Assisted Metabolic Mapping

DRI – Dorsal Raphe Interfascicular

DRN – Dorsal Raphe Nucleus

DRV – Dorsal Raphe Ventral

DRVL – Dorsal Raphe Ventro-lateral

DS – dorsal subiculum

DTg – dorsal tegmental nucleus

DVC – Dorsal Vagal Complex

EGFP – Enhanced Green Fluorescent Protein

Ent – entorhinal cortex

FDA – U.S. Food and Drug Administration

FDG – [18F]fluorodeoxyglucose

G proteins – Guanine Nucleotide Exchange Proteins

GABA – Gamma-Aminobutyric Acid

GAD – Generalized Anxiety Disorder

GAD – Glutamate Decarboxylase

GAD65 – 65-kD isoform of glutamic acid decarboxylase

GIRK – G Protein-Mediated Inwardly Rectified K+ channels

GPCR – G Protein Coupled Receptor

Hb – habenula

HCM – Home Cage Monitoring System

hM3Dq – Human Muscarinic 3 receptor DREADD coupling to Gq/11 proteins

hM4Di – Human Muscarinic 4 receptor DREADD coupling to Gi/o proteins

HPA – Hypothalamic-Pituitary-Adrenal

HVA – Homovanillic Acid

i.p. – Intraperitoneal Injections

IC – inferior colliculus

IS – Inactive States

L-5-HTP – L-5-hydroxytryptophan

LC – Light Cycle

LDTg – lateral dorsal tegmental nucleus

LO – lateral orbital cortex

MAOA – Mitochondrial Enzyme Monoamine Oxidase A

MAOI – Monoamine Oxidase Inhibitors

MC - primary motor cortex

mCPP – M-Chlorophenyl Piperazine

MPB – medial parabrachial nucleus

MR – Medial Raphe

MRGPRB4 – MAS-related GPR, member B4

MRN – Medial Raphe Nucleus

MT – medial thalamic nucleus

MVe – medial vestibular nucleus

NINDS – National Institute of Neurological Disorders and Stroke

NO – Novel Object

NPY – Neuropeptide Y

OCD – Obsessive Compulsive Disorder

PAG – periaqueductal grey

PBN – Parabrachial Nuclei

PBS – Phosphate Buffered Saline

PCPA – Para-Chlorophenylalanine

PFA – Paraformaldehyde

Pir – piriform cortex

POMC – Pro-opiomelanocortin

PTSD – Post-Traumatic Stress Disorder

PV – paraventricular nucleus of the thalamus

RFP – Red Fluorescent Protein

RMANOVA – Repeated Measures ANOVA

RSG – retrosplenial cortex

RTWANOVA – Regular Two-Way ANOVA

SC – primary somatosensory cortex

SERT – Serotonin Reuptake Transporter

Slc6a4 – Serotonin Reuptake Transporter Gene

SNP – Single Nucleotide Polymorphism

SNRI – Serotonin and Noradrenaline Reuptake Inhibitors

SPN – spinal trigeminal nuclei

SSRI – Serotonin Selective Uptake Inhibitors

SYN1 – Synapsin 1

TCA – Tricyclic Antidepressants

TH – thalamus

TPH – Tryptophan Hydroxylase

TPH1 – Tryptophan Hydroxylase 1

TPH2 – Tryptophan Hydroxylase 2

TTX – Tetrodotoxin

VC – visual cortex

VGLUT3 – Vesicular Glutamate Transporter Type 3

VMAT2 – Vesicular Monoamine Transporter Type 2

VMN – Ventromedial Nucleus

VN – vestibular nuclei

VO – ventral orbital cortex

LIST OF SYMBOLS

G_q - Gq type G protein alpha – stimulates phospholipase C

$G_{i/o}$ - Gi-type G protein alpha – inhibits adenylyl cyclase

G_s - Gs-type G protein alpha – stimulates adenylyl cyclase

Gβγ - G proteins beta and gamma

CHAPTER 1. INTRODUCTION

1.1. THE SEROTONIN NETWORK

1.1.1. Serotonin and Serotonin Receptors

Serotonin (5-hydroxytryptamine; 5-HT), is a neurotransmitter widely distributed

throughout the central nervous system (CNS) and periphery. While initially being

characterized as the active substance in rabbit brain extracts which caused peripheral

vasoconstriction (Rapport et al., 1948), it is now well known that serotonin can influence a

wide range of mammalian physiological processes from cardiovascular function and bowl

motility to the regulation of mood and perception (Berger et al., 2009; Lucki, 1998).

Serotonin achieves this broad modulation by tight cellular control over serotonin synthesis,

reuptake, and degradation in combination with an extensive serotonergic projection network

and interactions with numerous serotonin receptors. Synthesis of 5-HT begins with the rate

limiting hydroxylation of the amino acid L-tryptophan to L-5-hydroxytryptophan (L-5-HTP)

catalyzed by tryptophan hydroxylase (TPH). Two TPH enzymes, delineating two distinct

serotonin systems, have been identified, TPH1 and TPH2 (Walther et al., 2003). TPH1

generates 95% of the body's 5-HT, which is synthesized primarily in the gut and is

distributed to all organs except the brain (Filip and Bader, 2009). TPH2 is the rate-limiting

enzyme involved in the first step of serotonin synthesis in the CNS. Decarboxylation of L-5-

HTP occurs through L-amino acid decarboxylase converting L-5-HTP to 5-HT. Serotonin is taken up into secretory vesicles and transported to the presynaptic terminals of neurons, ready for release upon depolarization. Evidence suggests that vesicular monoamine transporter type 2 (VMAT2) plays an important role in this process (Hendricks et al., 2003; Hoffman et al., 1998).

A majority of serotonin released from neurons are thought to come from serotonergic varicosities, allowing the neurotransmitter to diffuse into extra neuronal space (Bunin and Wightman, 1998). Following release, the high-affinity serotonin reuptake transporter (SERT, 5-HTT, Slc6a4) removes serotonin from extracellular space and plays a prominent role in regulating extraneuronal serotonin concentrations (Torres and Amara, 2007). While reuptake is important for maintaining intracellular serotonin concentrations for continual release, it also allows for the degradation of serotonin through oxidative deamination by the mitochondrial enzyme monoamine oxidase A (MAOA) to form 5-hydroxyindole acetaldehyde. This is then oxidized by aldehyde dehydrogenase to form 5-hydroxyindole acetic acid (5HIAA), a major metabolite of serotonin.

In addition to its regulation, serotonin mediates its diverse effects through interactions with numerous receptors that have been classified into seven families: 5-HT1 - 5-HT7. These families are primarily comprised of seven transmembrane G protein coupled receptors which include 5-HT1, 5-HT2, and 5-HT4-5HT7 (Kroeze and Roth, 1998). The 5-HT3 receptor is the only ion channel that responds to serotonin and is permeable to cations (Peters et al., 1992). The 5-HT1 receptor family contains five members, labeled 5-HT1A, 5-HT1B, 5-HT1D, 5-HT1E, and 5-HT1F, and couples primarily to Gi/o G proteins involved in the inhibition of adenylyl cyclase. The 5-HT2 receptor family contains 3 members, labeled 5-

HT2A, 5-HT2B, and 5-HT2C, and is the only serotonin family that primarily couples to Gq

G proteins mediating calcium release through activation of phospholipase C and hydrolysis

of phosphoinositides. The 5-HT4, 5-HT6, and 5HT7 receptor families contain only one

member, although multiple splice variants exist for receptors 5-HT4 and 5HT7. All three of

these receptors signal primarily by coupling to Gs G proteins involved in activating adenylyl

cyclase. The 5-HT5 receptor family has two members, labeled 5-HT5A and 5-HT5B, both of

which primarily signal through coupling to Gi/o G proteins involved in the inhibition of

adenylyl cyclase. 5-HT5A is the only function member of this family expressed in humans,

while both 5-HT5A and 5HT5B are expressed in rodents (Rees et al., 1994). It is important to

note that these signaling pathways described here for each family are generalized primary

effector pathways. A multitude of evidence implicating additional unique primary and

secondary effector pathways for most members of these families have been shown, which

increases the complexity of serotonin-mediated signal transduction (Roth, 2006).

Additionally, all regions of the CNS express multiple members of serotonin receptor

families, which enable the modulation by serotonin of a wide variety of neuronal circuits and

thus physiology. For example, 5HT1A and 5HT2A receptors are both expressed in Layer V

pyramidal neurons in the cortex and differentially modulate pyramidal neuronal activity

(Araneda and Andrade, 1991), regulating higher cortical functions such as perception, and

cognition. In another example, 5HT1A and 5HT2C receptors have been found in the

amygdala and are both implicated in the contribution of serotonin-mediated stress responses

(Burghardt et al., 2007; Gonzalez et al., 1996), although 5-HT1A receptors have been shown

to reduce anxiety as well, most likely due to is expression on inhibitory GABA interneurons

as well as excitatory neurons (Cheng et al., 1998; Koyama et al., 2002). Given the wide

complexity of the serotonin system, it is not surprising that it is involved in virtually every mammalian behavior.

1.1.2. The Raphe Nucleus

The serotonin network stems from a group of nuclei termed the raphe. The serotonergic neurons in this relatively small group of nuclei (20,000-30,000 neurons in the rat CNS (Jacobs and Azmitia, 1992)) produce and release nearly all the serotonin in the CNS. They send ascending projections that terminate in an organized fashion throughout the cortical, limbic, midbrain, and hindbrain regions, and are thus ideally positioned to modulate the activity of a diverse set of mammalian neural circuits. Within the raphe, the serotonin neurons form distinct cell groups, initially described as the B1-B9 groups (Dahlstrom and Fuxe, 1964). These groups are clustered down the midline of the brain starting from the medulla, corresponding to the raphe pallidus, obscurus, and pontis (B1-B5), and continue rostrally into the pons and midbrain containing the dorsal raphe and medial raphe (B6-B9) (Lidov and Molliver, 1982; Steinbusch, 1981). Two broad subdivisions can be drawn along with their anatomical locations, in that the caudal raphe groups (B1-B5) generally send projections to the hindbrain, whereas the more rostral raphe groups (B6-B9) generally send projections to the forebrain (Lidov and Molliver, 1982). Ultrastructural analysis of these serotonin projections, or axons, revealed that they are primarily non-myelinated, implying slow serotonin neuronal transmission. Interestingly, a small portion of serotonin axons detected in the rostral regions in the medial forebrain bundle have been found to contain myelin, thus suggesting differential velocities of nerve conduction into the forebrain (Azmitia and Gannon, 1983). In addition, a majority of the terminal serotonergic axons do not form

4

synaptic specializations, although this varies according to brain structure. For example, in cerebral cortex and hippocampus, only 20% of serotonin terminals form synaptic junctions, whereas this increases to 50% in the substantia nigra and even to 75% when in the basolateral amygdala (Descarries, 2010; Muller et al., 2007). This work will primarily focus on the cells groups in the rostral raphe region that send projections into the cortical and limbic areas. The rostral raphe accounts for 85% of all the serotonergic neurons in the brain and is composed of two main subdivisions, the dorsal raphe (DR) (B6, B7) and the medial raphe (MR) (B8, B9) (Hornung, 2003). Even though these two cell groups have two distinct developmental origins (Jensen et al., 2008), their projections to the forebrain are parallel and largely overlapping, yet still retain specific regional distributions and cellular targets. The DR primarily innervates the cerebral cortex, striatum, amygdala, substantia nigra, hippocampus, locus coeruleus, entorhinal cortex, and thalamus, and to a lesser extent hindbrain regions such as the lateral tegmental area, superior colliculus, vestibular nuclei, the cerebellum and motor nuclei of the brain stem (Hornung, 2010). The MR primarily innervates the basal forebrain, septal region, ventral tegmental area, hypothalamus, midline thalamic nuclei, hippocampus, and to a lesser extent the cerebral cortex overlapping with the DR projections (Hornung, 2010). In addition, the MR contains hindbrain projections in the lateral dorsal tegmental nucleus and the cerebellum (Hornung, 2010). These two serotonin groups are further defined in that the DR axons have been shown to contain fine bead varicosities and do not form true chemical synapses, whereas MR axons have been shown to bear large, closely spaced varicosities and can be observed forming synapses (Hornung, 2003; Kosofsky and Molliver, 1987). The fact that these two groups in the rostral raphe give rise to similar, yet distinct innervation patterns and axons fibers, allows the potential to selectively dissect this

5

complex system in order to determine how each subdivision contributes to the modulation

neural circuitry and mammalian physiology.

1.1.3. The Serotonergic Neurons of the Dorsal Raphe Nucleus

The dorsal raphe nucleus contains the largest group of serotonergic neurons,

accounting for about one third of all serotonergic neurons in the brain. Most serotonin

neurons are located in the rostral half and can be subdivided into four main regions: the

dorsal (DRD), the ventral (DRV), the interfascicular (DRI), and the ventro-lateral (DRVL)

(Baker et al., 1990). Other serotonin neurons extend laterally into the ventral periaqueductal

grey area and surround the medial longitudinal fasciculus. Finally, serotonin neurons are also

present in the caudal subdivision (DRC) at the boarder of the hindbrain. It is important to

note that not all neurons in the dorsal raphe are serotonergic. In most subdivisions of the

dorsal raphe, 50-60% of neurons are serotoninergic. This number increases to 80% for the

DRV and to 100% for DRI (Hornung, 2010). Serotonin-specific projections from the DR are

spread widely throughout the forebrain and are organized based on their location, such that

the more rostral serotonergic neurons project selectively to specific sites such as the

neocortex, caudate putamen, and substantia nigra, whereas the more caudal serotonin neurons

project to areas such as the hippocampus and entorhinal cortex (Abrams et al., 2004).

Furthermore, individual serotonin neurons have been shown to contain collateralized or

branched projections to anatomically distinct areas (Lowry, 2002), creating additional

complexity and suggesting the possibility that a few serotonin neurons may modulate

multiple neuronal circuits. In addition, considerable diversity exists within the DR nucleus

with respect to serotonin cell morphology and electrophysiological properties (Calizo et al.,

6

2011; Descarries et al., 1982; Steinbusch et al., 1981), suggesting the possibility that further subdivisions could be made based on these properties as well as location, which may ultimately lead to the identification of discrete serotonergic groups with defined roles in neural circuitry (Ray et al., 2011). Figure 1 reveals the large diversity of serotonergic projections stemming from the dorsal raphe generated by utilizing a Cre-dependent fluorescent neuronal tracer injected into the dorsal raphe of the Slc6a4-Cre mouse line. These regions range from the cerebral cortex, caudate putamen, amygdala, thalamus and olfactory bulb, to the cerebellar and motor nuclei in the brain stem (Fig. 2).

1.1.4. Serotonergic Regulation of the Dorsal Raphe

Due to the broad range of neural circuits that are influenced by the serotonin network, it is not surprising that negative feedback mechanisms provide a tight regulatory system that maintains a homeostatic tone for proper serotonergic function. The discovery of this negative feedback system arose from a series of experiments demonstrating that 5-HT and 5-HT receptor agonists inhibited raphe firing and the release of radiolabeled 5-HT (Aghajanian et al., 1972; Farnebo and Hamberger, 1971; Gothert and Weinheimer, 1979), suggesting the presence of 5-HT autoreceptors that act at the somatodendrites and nerve terminals to inhibit transmission. In addition, this negative feedback regulation is supported by the presence of 5-HT axon terminals in the dorsal raphe (Descarries et al., 1982) as well as by work suggesting the presence of a 5-HT axon collateral inhibitory mechanism (Wang and Aghajanian, 1977). Furthermore, increasing extracellular serotonin by administrating compounds that block 5-HT reuptake (i.e. SSRIs) results in the inhibition of serotonin synthesis (Barton and Hutson, 1999) and release (Adell and Artigas, 1991; Hjorth and Auerbach, 1994). The primary

7

serotonin autoreceptor implicated in these negative feedback studies is the 5-HT1A receptor found on the soma and dendrites of serotonin neurons. Agonist-induced stimulation of the 5-HT1A receptor in the dorsal raphe hyperpolarizes and dampens neuronal activity through its activation of G protein-mediated inwardly rectified (GIRK) K+ channels mediated by interactions with G protein $\beta\gamma$ subunits (Doupnik et al., 1997; Penington et al., 1993). Another population of 5-HT autoreceptors is the 5-HT1B receptor, which has been located on axon terminals allowing it to directly inhibit serotonin release (Davidson and Stamford, 1995; Middlemiss and Hutson, 1990). In addition, while the contribution may be small, the 5-HT1D receptor has also been shown to modulate 5-HT release at dendrites and axons (Pineyro and Blier, 1996; Stamford et al., 2000).

While this work focuses on the modulation of behavioral neural processes by serotonin, it is important to mention that a large driving force of DR activity is generated by afferent projections from multiple areas in the brain. These include the lateral habenula, interpeduncular nucleus, certain hypothalamic nuclei, ventral tegmental nuclei, lateraldorsal tegmental nuclei, cingulate cortex, medial prefrontal cortex, and the central amygdala (Behzadi et al., 1990; Hajos et al., 1998; Peyron et al., 1998). While these are primarily made of glutamatergic afferents, there are also numerous inhibitory GABAergic innervation of the DR (Wang et al., 1992).

1.1.5. Other Neurotransmitters and Peptides in the Dorsal Raphe

Extensive studies of the dorsal raphe have revealed a multitude of neuropeptides and neurotransmitters other than serotonin that reside in this nucleus. For example, neuropeptides such as substance P (Baker et al., 1991; Hokfelt et al., 1978), enkephalin (Hokfelt et al.,

1977), corticotropin-releasing factor (CRF) (Commons et al., 2003; Day et al., 2004), and neurotensin (Jennes et al., 1982) have been shown in neurons within the DRN. In addition, evidence suggesting neurotransmitters such as dopamine (Ochi and Shimizu, 1978), GABA, and glutamate (Calizo et al., 2011; Fu et al., 2010) have also been shown to be present in the dorsal raphe nucleus and modulate serotonergic function in the raphe. The question of whether any of these signaling molecules overlap with serotonin neurons has been frequently investigated. While previous studies have suggested a large co-localized population exists with substance P (Baker et al., 1991) and to a lesser degree with CRF (Commons et al., 2003; Day et al., 2004) in rats, a recent study in mice reveals the lack of co-localization of a number of neuropeptides, including substance P, cholecystokinin, enkephalin, somatostatin, neurotensin, dynorphin, thyrotropin-releasing hormone, and CRF as well as the neurotransmitter dopamine (Fu et al., 2010). While there is evidence of glutamate decarboxylase (GAD) in a few 5-HT neurons (Hioki et al., 2009), the atypical vesicular glutamate transporter VGLUT3 has been shown to overlap with many serotonin-containing neurons (Gras et al., 2002; Hioki et al., 2009). Incidentally, even though VGLUT3 is co-expressed with serotonin, no evidence has surfaced demonstrating that glutamate is actually released from serotonin neurons. In summary, while the dorsal raphe is made up of a heterogeneous mix of neurons producing and responding to a wide range of neuropeptides and neurotransmitters, serotonin neurons seem to be a distinct population in mice, but this does not exclude the possibility that they modulate the activity of serotonin neurons.

1.2. MODULATION OF ANXIETY, DEPRESSION, AND FEEDING BY SEROTONIN

While serotonin can affect virtually all mammalian behaviors, this study will focus on its modulation of three psychological disorders: anxiety, depression, and eating. Dysfunction of the serotonergic network and neurotransmission has been associated with the three aforementioned disorders (Graeff et al., 1997; Levy and Van de Kar, 1992). The following subchapters of this work will briefly describe the role of serotonin in these disorders and serotonin-targeted medications as a treatment of these disorders.

1.2.1. Serotonin and Anxiety

Anxiety can be described as the body's response to real or imagined aversive stimuli. Many CNS circuits and structures are involved in the response to psychologically and physically aversive stimuli. For example, stress and anxiety can stimulate the hypothalamic-pituitary-adrenal (HPA) axis, which leads to rapid release of the adrenocorticotropin hormone (ACTH) from corticotrophs in the anterior pituitary and thus an increase in the circulation of corticosteroids, initiating the "fight or flight" response (Carrasco and Van de Kar, 2003). CRF, while not solely responsible, releases ACTH from the pituitary gland, suggesting that it plays a role in mediating the responses to stress and anxiety (Binder and Nemeroff, 2010). The fact that CRF-immunoreactive fibers have been found innervating the dorsal raphe, combined with evidence demonstrating that urocortin 2, an agonist of CRF receptors, activates serotonergic neurons in the dorsal raphe, suggests that serotonin has a role in stress-related responses (Staub et al., 2006; Staub et al., 2005; Valentino et al., 2001). In fact, serotonergic neurons in the dorsal raphe were activated in response to a number of

anxiogenic drugs, including the benozodiazepine inverse agonist FG-7142, the alpha2-adrenoceptor antagonist yohimbine, the non-selective 5-HT2C receptor agonist m-chlorophenyl piperazine (mCPP), and the adenosine antagonist caffeine (Abrams et al., 2005; Singewald and Sharp, 2000). In addition, uncontrollable stress has been shown to increase the activity of serotonergic neurons in the dorsal raphe (Amat et al., 2005; Grahn et al., 1999). Increases in serotonergic activity and its implication in anxiety states can be further explained by dorsal raphe serotonergic innervation of two key anxiety centers: the amygdala and the bed nucleus of the striatum terminalis (Commons et al., 2003; Li et al., 1990). It is important to note that differential changes in serotonin concentrations in different regions of the brain after various types of stress have been observed, suggesting a more complex regulation of the stress response by serotonergic activity (Amat et al., 1998a; Amat et al., 1998b; Kirby et al., 1995; Rueter et al., 1997). Nevertheless, acute increases in serotonin through blockade of serotonin reuptake inhibitors have been shown to exacerbate anxiety in patients and in mouse models (Nierenberg et al., 2000; To et al., 1999). These results corroborate observations that anxiogenic behaviors in mice occur following the artificial elevation of serotonin levels through administration of high doses of 5-HTP (Artaiz et al., 1998). In summary, increasing serotonergic activity, whether by stressful events or anxiogenic drugs, is involved in mediating the physiological responses to anxiety and stress.

Because serotonin is implicated in the response to anxiety and its dysfunction is associated with anxiety disorders, therapeutics that modulate the serotonin network are frequently prescribed to treat these disorders. Small molecules ranging from tricyclic antidepressants (TCA), monoamine oxidase inhibitors (MAOI), and serotonin-selective reuptake inhibitors (SSRI), are used as first- and second-line treatment for a variety of

anxiety disorders, including generalized anxiety disorder (GAD), panic, social anxiety, post-traumatic stress disorder (PTSD), and obsessive compulsive disorder (OCD) (Stahl, 2008). Medications that increase serotonin levels, such as SSRIs, MAOIs, and TCAs, may seem contradictory due to the exacerbation of anxiogenic responses as mentioned above, but surprisingly, long-term or chronic treatments with these drugs are very efficacious (Den Boer and Westenberg, 1990; den Boer et al., 1987; Gorman et al., 1987). In addition, chronic treatment with SSRIs abolishes the anxiogenic effects of endocrine, social and conditioned stress in animal models (To et al., 1999; To and Bagdy, 1999; Zhang et al., 2000). Multiple theories have been constructed in an attempt to resolve this bi-phasic response of increased serotonin and its differential regulation of anxiety. Desensitization of autoreceptors such as 5-HT1A, together with the down regulation of G proteins, have been proposed as a critical step for anxiolytic efficacy with SSRIs (Hensler, 2002; Lerer et al., 1999; Li et al., 1996; Raap et al., 1999). While the available evidence supports this claim, long-term increases in serotonin, enabling the modulation of numerous neural circuits, mostly likely will result in the global remodeling of these circuits in order to adapt to this perturbation. At the moment, the changes induced by chronically increasing serotonin are still poorly understood and studies investigating how networks adapt due to this treatment are needed.

1.2.2. Serotonin and Depression

Depression refers to a heterogeneous group of psychological disorders characterized by similar symptoms that most likely originate from different abnormalities in various neural circuits. The official diagnosis of depression is still very subjective and relies on the characterization of a certain number of functionally impairing symptoms (Nestler et al.,

2002). These symptoms overlap with other disorders such as anxiety, which can have substantial co-morbidity (Hasler et al., 2004; Stahl, 2008). Early attempts to describe the biological etiology of these disorders gave rise to the hypothesis that depression is due to a deficiency of monoamine neurotransmitters such as serotonin. Currently, direct evidence for this hypothesis is lacking even though a great deal of effort has been made to identify this deficiency. Nevertheless, multiple abnormalities in serotonergic neurotransmission have been described in patients with major depression, leading to the revised hypothesis that altered serotoninergic activity is a risk factor rather than the underlying cause for this complex spectrum of disorders (Maes, 1995). In support of this hypothesis, reports of decreased 5-HT, 5-HT neurons, and dorsal raphe size in depressed suicide victims have been shown in some studies (Matthews and Harrison, ; Shaw et al., 1967). Furthermore, 5-HT depletion studies, whether by dietary restriction or by treatment with the tryptophan hydroxylase inhibitor para-chlorophenylalanine (PCPA), has led to clinical relapses of depression in patients and has decreased the mood of healthy controls (Shopsin et al., 1976; Shopsin et al., 1975; Young et al., 1985). Finally, a single nucleotide polymorphism (SNP) (G1463A) in TPH2 was found in a small subset of patients with major depression, and was demonstrated to reduce functionality of the enzyme by 80% (Zhang et al., 2005). Analysis of this SNP in a knock-in mouse (TPH2-R441H) revealed a reduction in 5-HT and 5-HT synthesis, increased depression- and anxiety-like behaviors, along with depression-like biomarkers such as low CSF 5-HIAA and increased expression of 5HT2A in the frontal cortex (Beaulieu et al., 2008; Jacobsen et al., 2012). In summary, dysfunction of the serotonergic system is clearly implicated in depression and depressive-like symptoms, even though it may not be the underlying cause for this group of disorders.

Similar to its role in anxiety, serotonin also plays a role in the etiology and therapy of the depression spectrum. Many similar medications used to treat anxiety are also employed as first- and second-line treatments for depression (Stahl, 2008). As with anxiety, several weeks of treatment are required for improvement in depressive-like symptoms (Nurnberg et al., 1999). While it is well documented that chronic administration of these antidepressants increases serotonin neurotransmission (Blier and de Montigny, 1994; Kreiss and Lucki, 1995; Moret and Briley, 1996), it is hypothesized that this increase produces secondary neuroplastic changes that occur on a longer time and are critical for antidepressant efficiency. One example of a neuroadaptive change that is thought to be critical for increasing 5-HT concentrations, and therefore the actions of antidepressants, is the desensitization of autoreceptors (McDevitt and Neumaier, 2012). While there is extensive evidence that these drugs initiate this desensitization, perhaps the most striking evidence for this hypothesis is the increase in antidepressant onset obtained after co-administration of the 5-HT1A/beta-adrenergic antagonist pindolol with SSRIs (Blier, 2003). Other neuroadaptive changes have been proposed as a result of antidepressant treatment, including increases in brain-derived neurotrophic factor (BDNF), cyclic-AMP-response-element-binding protein (CREB), histone acetylation, and neurogenesis (Krishnan and Nestler, 2008). While these changes may play a role in the response and actions of antidepressants, studies that investigate how chronic increases in serotonin alter overall network activity are needed to better understand the delayed onset of efficacy.

1.2.3. Serotonin and Feeding

Feeding behaviors are comprised of a diverse, complex set of neural circuits and peripheral hormones that regulate different aspects of ingestive behaviors such as meal initiation, meal termination, and satiety. Serotonin has been implicated in the regulation of feeding behaviors as demonstrated by early studies observing an induction of hyperphagia when 5-HT levels were decreased and hypophagia when 5-HT levels were increased (Fletcher and Paterson, 1989; Saller and Stricker, 1976). In fact, serotonergic dysregulation has been demonstrated in various eating disorders, which exhibit comorbidity with depression (Brewerton, 1995; Jimerson et al., 1990). It is well known that the hypothalamus is a key site of integration of multiple central and peripheral signals. Small populations of peptidergic neurons, such as the pro-opiomelanocortin (POMC), cocaine and amphetamine regulated transcript (CART), agouti-related protein (AgRP) and neuropeptide Y (NPY)-containing neurons, within the hypothalamus form intricate feeding circuits that regulate behavioral responses to food intake. Recently it has been shown that the serotonin system can influence two important sets of neurons within the arcuate nucleus of the hypothalamus, POMC/CART and AgRP/NPY neurons. Serotonin can simultaneously reduce the activity of AgRP/NPY neurons through activation of 5-HT1B receptors while inducing depolarization of POMC/CART neurons through the activity of 5-HT2C receptors, thus resulting in large reductions in food intake (Heisler et al., 2002; Heisler et al., 2006). In addition to this circuit, other feeding centers have also been implicated in the anorexic effects of increased serotonin, such as the dorsal vagal complex (DVC) and the parabrachial nuclei (PBN) within the brain stem (Tecott, 2007). Serotonin can modulate food intake and therefore energy balance at many points in these complex circuits that govern feeding behaviors.

Given that increasing serotonin concentrations in the brain has proven to be effective in attenuating food intake, manipulation of the serotonergic system has been an ongoing target of anti-obesity pharmacotherapies. Serotonin induced weight loss was initially investigated using medications that augmented serotonin concentrations throughout the brain, such as 5-HTP, SSRIs, serotonin and noradrenaline reuptake inhibitors (SNRIs) and fenfluramine (disrupts 5-HT vesicle storage and reverses SERT function) (Brown et al., 2001; Fletcher and Burton, 1986; Yen, 1987). All of these therapeutics have demonstrates significant weight loss in clinical trials and some have even gained FDA approval (fenfluramine, its more efficacious enantiomer dexfenfluramine, and sibutramine) (Halford et al., 2007). Due to safety concerns, such as off target effects at the "death receptor" 5-HT2B that induce valvulopathies (Rothman et al., 2000), most have been withdrawn from clinical use. Despite the withdrawal of these medications, they have led to the investigation of more targeted therapies primarily through studies demonstrating that the action of fenfluramine at 5HT2C and 5HT1B receptors are required for its influence on ingestive behaviors (Lucas et al., 1998; Vickers et al., 1999). These studies, and the observation that 5-HT2C knockout mice have increased food intake and weight gain (Tecott et al., 1995), have led to the investigation of 5-HTC-specific compounds to induce weight loss. Arena pharmaceuticals recently obtained FDA approval for their 5-HT2C agonist, lorcaserin, for the treatment of obesity. In addition, the FDA recently placed lorcaserin as a Schedule IV drug, highlighting the abuse potential due to its 5-HT2A receptor affinity and illustrating the difficulty involved in designing selective serotonin receptor therapeutics for weight loss. Additionally, serotonin can greatly influence the diurnal cycle, which is intricately connected to feeding behaviors (Leibowitz and Alexander, 1998). In fact, chronic administration of serotonin into the

ventromedial nucleus (VMN) of the hypothalamus causes reciprocal feeding behaviors depending on the diurnal cycle such that no overall weight loss is achieved in obese rats (Fetissov and Meguid, 2010). Further research into how these two systems interact may yield more effective serotonin-mediated treatment paradigms.

1.3. SELECTIVE CONTROL OF THE SEROTONIN NETWORK

The previous subchapters of this work have attempted to convey the magnitude and the complexity of the serotonin system and its influences on multiple physiological and psychological processes. Prior work has demonstrated significant progress towards elucidating the functionality of the serotonin network through the study of its receptors, projection areas, and sites of synthesis. Nevertheless, studies dividing this system into its parts by selectively and reversibly controlling specific regions of the serotonin network may lead to a greater understanding of how it can influence so many different processes and in addition generate new hypotheses for more targeted therapies. One way to achieve this is to dissect the raphe nuclei into its subdivisions with the goal of potentially identifying discrete groups of 5-HT neurons that are responsible for regulating different serotonergic-mediated processes. This approach has been challenging in the past and was limited to lesions or systemic and/or direct application of compounds known to induce serotonergic activity. These methods, while providing insight into the function of the raphe, lacked specificity and selectivity. Recently, new techniques have been shown to provide selective and bi-directional control over many different types of neuronal signaling and are revolutionizing neural physiology (Alexander et al., 2009; Armbruster et al., 2007; Boyden et al., 2005). Some of these novel approaches have targeted the raphe, but unfortunately have either lacked

serotonin selectivity or failed to differentiate the specific serotonergic nuclei in the raphe (Guler et al., 2012; Ray et al., 2011; Warden et al., 2012). With the increasing number of molecular tools available for neurophysiology and neuropharmacology, serotonin research is poised to make great strides in elucidating these complex neural networks.

1.4. PHARMACOSYNTHETICS

Pharmacosynthetics, is defined as "a branch of biology which deals with the creation of pharmacological modulation using artificial components" (Farrell and Roth, 2012). This terminology refers to novel designer receptors created to probe cellular signaling and their effects on physiology. These receptors were generated to address potential confounds when investigating the physiological role of native signaling receptors, like GPCRs, that have expression profiles throughout multiple tissues and cell types. This experimental system (also referred to as chemogenetics) now allows for the activation of a particular type of signaling pathway in a specific cell type and/or tissue, thus providing a greater understating of how it may affect the physiology of the organism.

1.4.1. Designer Receptor Exclusively Activated by Designer Drug (DREADD) Technology

DREADDs are G protein-coupled receptors (GPCRs) containing alterations in their amino acid sequence in order to confer insensitivity to their native ligand and responsiveness to an exogenous pharmacologically inert ligand. They were derived from the muscarinic class of GPCRs and contain two mutations (Y3.33C and A5.46G) of two highly conserved residues in the third and fifth transmembrane regions. These two mutations, residing in the

muscarinic orthosteric-binding pocket (Wess et al., 2013), are enough to shift the dose

response curve of the highly potent endogenous ligand, acetylcholine (ACh), far enough to

right that it is essentially inactive at the receptor, thus generating a native GPCR with no

endogenous ligand. Simultaneously, these two mutations also shift the dose-response curve

of the weak partial agonist clozapine-N-oxide (CNO), a pharmacologically inert metabolite

of clozapine, to a potent full agonist, thus generating an extremely selective, highly potent

exogenous ligand (Armbruster et al., 2007; Weiner et al., 2004). Using this manipulation

with the human muscarinic 3 and 4 receptors, DREADDs were produced that coupled to Gq

and Gi G proteins respectively. Due to the lack of a native Gs-coupling muscarinic receptor,

a chimera was created by exchanging intracellular loops two and three for those of the Gs-

coupled β1-adrenergic receptor (Guettier et al., 2009). Extensive validation of signal

transduction, desensitization, and internalization have demonstrated that these DREADDs are

nearly identical to their non-mutant muscarinic counterparts (Alvarez-Curto et al., 2011;

Armbruster et al., 2007; Conklin et al., 2008; Guettier et al., 2009; Kaufmann et al., 2013;

Nawaratne et al., 2008). Combined, these orthologous ligand-GPCR pairs represent a

significant advancement as tools for manipulating GPCR signaling in virtually every

mammalian system.

1.4.2. Modulation of neuronal activity through DREADD activation

GPCR signaling mediates a diverse range of cellular responses including

proliferation, differentiation, and contraction. In addition, it has been well established that

GPCR-induced signal transduction pathways have the ability to modulate neuronal activity in

the CNS (Roth, 2006). Thus, manipulation of these signal transduction pathways can provide

control over neuronal signaling and insight into how this signaling translates into behavioral phenotypes. As mentioned above, DREADDs can deliver this control and have been shown to selectively, reversibly, and bi-directionally influence neuronal activity. The hM3Dq (h = human, M3 = muscarinic 3 receptor, D = DREADD, and q = coupling to Gq/11 proteins) mediates neuronal excitation through a phospholipase C-dependent manner potentially involved in the closing of potassium channels (Alexander et al., 2009), while the hM4Di (h = human, M4 = muscarinic 4 receptor, D = DREADD, and i = coupling to Gi/o proteins) mediates neuronal silencing through Gβγ activation of GIRK channels (Armbruster et al., 2007). Extensive in vivo validation of the capacities of hM3Dq and hM4Di receptors to modulation neuronal signaling has been demonstrated recently (refer to Table 1). While canonical G protein-mediated signaling cascades are initiated through the activation of these designer receptors and can lead to a wide variety of cellular effects such modulation of transcription and gene expression, most of these studies have utilized this technology to either activate or silence neurons in a cell-type and tissue selective fashion.

1.4.3. Deconstruction of complex neuronal circuits using DREADDs

DREADDs have become a powerful tool to map neuronal circuitry, allowing neuroscientists to address how signaling at the cellular level can give rise to alterations in neuronal networks and ultimately changes in mammalian physiology and behavior. Cell-type and tissue-specific expression of these receptors are critical for deconstructing and probing these circuits. Cell-type and tissue-specific expression in animal models can be achieved through many different approaches (Farrell and Roth, 2012; Rogan and Roth, 2011; Wess et al., 2013). This work will briefly discuss the utility and versatility of combining Cre mouse

driver lines with Cre-sensitive viruses. Cre mouse driver lines have distinct cell-type and

tissue-specific expression patterns of Cre recombinase (Cre), a tyrosine recombinase enzyme,

due to the transgenic insertion of Cre after specific promoters of a wide variety of genes.

While these driver lines were initially used for the cell-type removal of various genes when

crossed with cre-dependent knock-out mouse models, recently these lines been have been

combined with cre-sensitive viruses in order to gain a more selective cell-type and tissue-

specific expression. Cre-sensitive viruses are created by surrounding an inverted gene (i.e.

DREADD) with two pairs of heterotypic, antiparallel loxP sites (designated LoxP and

Lox2722) (Fig. 3A). Without Cre expression, the DREADD cannot express due to it inverted

orientation. Upon infection of Cre containing cells, the DREADD gene is restored to its

proper orientation and expression occurs (Fig. 3A). Stereotaxic injection of these

recombinant viruses allows for further tissue-selectivity and is a commonly used delivery

mechanism. This approach has been utilized for selective control over Orexin neurons in the

lateral hypothalamus, AgRP, POMC, and RipII expressing neurons in the arcuate nucleus,

striatonigral and stritopallidal medium spiny neurons of the striatum, MRGPRB4 (MAS-

related GPR, member B4) sensory neurons, somatotstatin-postive neurons of the central

amygdala, parvalbumin-containing neurons in the binocular zone of primary visual cortex,

granule neurons of the olfactory system, and CAMKIIa-containing neurons of the orbital

frontal cortex (Table 1). Additionally, this technique can be used to isolate subdivisions of

neurotransmitter systems to determine the contribution of each nucleus and how it modulates

the network. For example, using a Slc4a6-Cre mouse line, in which serotonin reuptake

transporter (SERT) is predominately expressed in serotonergic neurons in the raphe nucleus,

injection of viruses encoding either the hM3Dq or hM4Di receptor into the dorsal raphe

would provide the capacity to activate or silence serotonergic neurotransmission in regions that are specifically innervated by serotonin neurons of the DRN. This type of manipulation allows for insight into how these neurons can modulate global neural networks in order to induce physiological changes such in behavior. Furthermore, this manipulation allows for the study of differential temporal modulation of selective neuronal populations, providing insight into how networks remodel as a result of continuous perturbations, mimicking chronic drug treatments. While more selective expression and control will be needed for future studies this would represent the initial step in the dissection of a complex neurotransmitter network.

CHAPTER 2. A BEHAVIORAL PROGRAM AND NEURAL NETWORK ENCODED BY DORSAL RAPHE SEROTONERGIC NEURONS.

2.1. INTRODUCTION

The central nervous system (CNS) serotonergic network is a large and complex efferent system that impacts a highly diverse range of behavioral and physiological processes, including mood, anxiety, food intake, and energy expenditure (Berger et al., 2009). Serotonergic neurons are distributed in a series of predominantly midline raphe nuclei extending from the midbrain to the caudal medulla, and projecting widely throughout the brain and spinal cord (Jacobs and Azmitia, 1992). The CNS serotonin (5-hydroxytryptamine; 5-HT) system has long been a major focus for CNS drug development, and its pharmacological modulation has been proposed to contribute to the therapeutic actions of medications used for a wide range of mood and behavioral disorders (Berger et al., 2009). Because some of the most commonly prescribed serotonergic drugs, such as 5-HT selective reuptake inhibitors (SSRI's), have a global impact on serotonergic neurotransmission, the serotonergic neuronal mechanism(s) responsible for both their therapeutic and adverse effects have been difficult to discern. Achieving selective control over specific serotoninergic nuclei could begin to elucidate these neural mechanisms as well as dissect 5-HT's influence over the diverse behavioral and physiological processes with which it is associated.

The midbrain dorsal raphe nucleus (DRN) is the largest of the raphe nuclei, and DRN

serotonergic neurons project rostrally to provide the predominant serotonergic innervation of the forebrain (Jacobs and Azmitia, 1992; Vertes, 1991; Waselus et al., 2012). Accordingly, dysregulation of DRN serotonergic neurotransmission has been implicated in psychiatric illnesses, such as anxiety and depression (Graeff et al., 1996; Lowry et al., 2008; Underwood et al., 1999) and the modulation of 5-HT release from DRN projections has been proposed as being critical for antidepressant efficacy (Stamford et al., 2000). While the selective manipulation of DRN serotonergic neurons could theoretically illuminate these processes, this has proven difficult since many (50-75%) neurons in the DRN are non-serotonergic (Halberstadt and Balaban, 2008).

The ability to selectively modulate both acute and chronic activity of distinct serotonergic neuronal subpopulations would provide a powerful approach for unraveling neural pathways and mechanisms relevant to mood and behavioral disorders. Designer receptors exclusively activated by designer drugs (DREADDs) are uniquely suited for this type of neuronal manipulation (Alexander et al., 2009; Armbruster et al., 2007). These evolved GPCRs can modulate both short- and long-term neuronal activity, mimicking drug-like actions (Rogan and Roth, 2011; Wess et al., 2013). DREADDs are thus ideal for selectively stimulating or inhibiting subpopulations of neurons and represent a non-invasive, reliable, reversible, and inducible approach for probing serotonergic function in behaving laboratory animals.

Because the hM3Dq DREADD reversibly augments neuronal activity (Alexander et al., 2009; Krashes et al., 2011), we selectively expressed it in DRN serotonergic neurons and then mapped the behavioral and neural alterations induced by acute and chronic stimulation. A high-resolution, quantitative behavioral analysis approach revealed alterations in feeding

patterns indicative of a previously unappreciated circadian influence on the serotonergic regulation of feeding behavior. These studies further revealed that acute and chronic activation of DRN serotonergic neurons are sufficient to induce behavioral effects across multiple assays that resemble both the acute and chronic responses to SSRI antidepressants. Finally, we mapped changes in whole-brain metabolic activity induced by activating DRN serotonin neurons in behaving mice using DREAMM (DREADD-assisted metabolic mapping; (Michaelides et al., 2013)). Altogether, these findings reveal a diversity of processes by which DRN serotonergic neurons modulate network activity relevant to therapeutic effects.

2.2. METHODS

Clozapine-N-Oxide (CNO). CNO was obtained from NIH as a part of a Rapid Access to Investigative Drug Program funded by the National Institute of Neurological Disorders and Stroke (NINDS). For all in vivo experiments, CNO was first dissolved in DMSO, and then brought to a final concentration with 0.9% saline at a concentration of DMSO at 0.4%. For all in vivo experiments, the appropriate vehicle controls (0.4% DMSO in saline) were utilized. A dose of 2 mg/kg was used for acute treatment (i.p.) at a volume 100 µl/10 g body weight. Chronic treatment consisted of 3-4 weeks of 5 mg/kg/day administered in the drinking water. The water bottles were protected from light and changed every 3 to 5 days. For microdialysis, an acute dose of 3 mg/kg (i.p.) was used.

Animal Subjects. General Procedure. All procedures were conducted in accordance with the Guide for the Care and Use of Laboratory Animals, as adopted by the National Institutes of Health, and with approval of the Institutional Animal Care and Use Committees

at the University of North Carolina (UNC), Duke University, and the University of California at San Francisco. Adult, age-matched, male Slc6a4-Cre mice (MMRRC: Stock number – 017260UCD) were used for all in vivo and ex-vivo experiments.

Generation of Slc6a4-hM3Dq and Slc6a4-EGFP mice. Adult (22–30 g) Slc6a4-Cre males (MMRRC : Stock number – 017260UCD) were group-housed before surgery. Unless described otherwise, all mice were maintained on a standard 12-h light/dark cycle (lights off at 7:00) with ad libitum access to food and water. Mice were anaesthetized with a ketamine (100 mg/kg body weight) and xylazine (10 mg/kg) solution and placed into a stereotaxtic frame (Kopf Instruments). For all experiments, male mice were bilaterally injected with 0.75 – 1 μl (depending on viral titer) of purified and concentrated adeno-associated virus (AAV) (~10^{12} infections units/ml, packaged in serotype 8 by the UNC Vector Core Facility) into the dorsal raphe using the following stereotaxtic coordinates: -4.6 mm to bregma, ±1.93 mm lateral to midline, and −3.46 mm ventral to the skull surface at an angle of 30°. Dorsal raphe neurons were transduced with virus encoding the hM3Dq-mCherry or EGFP in reverse orientation floxed by two lox sites (lox P and lox 2722) under the control of the human synapsin (SYN1) promoter. Following surgery, the mice were individually housed and monitored for signs of complications until they recovered from surgery. We performed all experiments 4-16 weeks after surgery. All viral constructs were packaged by the UNC Vector Core Facility at a final working concentration of 4×10^{12} to 6×10^{12} genome copies/ml. After all experiments, every mouse was perfused and the dorsal raphe subjected to immunohistochemistry to validate injection efficiency and viral expression.

Immunohistochemistry. Mice were anaesthetized with tribromoethanol (Avertin) and then transcardially perfused with 20 mL phosphate-buffered saline (PBS; pH 7.4) followed

by 4% paraformaldehyde (PFA) in PBS. Brains were dissected, postfixed overnight at 4oC in 4% PFA, followed by dehydration in a 30% sucrose (w/v) solution in PBS for 48 hrs. Brain sections were permeabilized for 20 min with 0.3% Trition X-100 in PBS and blocked for 1 hr at room temperature RT) in blocking buffer (PBS containing 0.3% Trition X-100, 2% normal goat serum, and 3% bovine serum albumin). Slides containing sections from mice infected with hM3Dq-mCherry virus were incubated with mouse monoclonal anti-RFP (1:1000 ab65856 – Abcam, Cambridge, MA) and rabbit polyclonal anti-5-HT (1:500 (20080 – Immunostar, Husdon, WI) (for cell bodies) and 1:5000 (S5545 - Sigma Aldrich, St. Louis MO) (for axons) in blocking buffer overnight at 4°C. Slides containing sections from mice infected with EGFP virus were incubated with mouse monoclonal anti-GFP (1:500 ab1218 – Abcam, Cambridge, MA) in blocking buffer for 48 hrs at 4°C followed by addition of polyclonal anti-5-HT (1:500 Immunostar – 20080) and further incubated overnight at 4°C. Slides were washed 4 times with PBS containing 0.3% Trition X-100 followed by a 1 hr incubation at RT with secondary fluorescent-conjugated antibodies in blocking buffer. Secondary antibodies used were: goat anti-rabbit AlexaFluor-488, goat anti-rabbit AlexaFluor-594, goat anti-mouse AlexaFluor-488, and goat anti-mouse AlexaFluor-594 (1:250, Invitrogen, Carlsbad, CA). After an additional 3 washes in PBS containing 0.3% Trition X-100, slides were mounted and fluorescent images were collected on either a Nikon 80i Research Upright Microscope (Nikon, Tokyo, Japan) equipped with Surveyor Software with TurboScan (Objective Imaging, Kansasville, WI) or an Olympus Fluoview FV1000 Laser Scanning Confocal Microscope (Olympus, Center Valley, PA). Tiled images were collected with a Qimaging Retiga-EXi camera (Qimaging, Surrey, BC, Canada). For co-localization studies, images of coronal slices were analyzed using ImageJ software (NIH).

Electrophysiology. Mice were decapitated under isofluorane anesthesia. Their brains were rapidly removed and immediately placed in a solution of ice-cold sucrose-artificial cerebrospinal fluid (aCSF) [(in mM): 194 sucrose, 20 NaCl, 4.4 KCl, 2 CaCl2, 1 MgCl2, 1.2 NaH2PO4 , 10 glucose, and 26 NaHCO3 saturated with 95% O2/5% CO2]. Brains were sectioned at 0.06 (mm/s) on a Leica 1200S vibratome to obtain 300 μm coronal slices of the dorsal raphe, which were incubated in a heated holding chamber containing normal, oxygenated aCSF [(in mM):124 NaCl, 4.4 KCl, 2 CaCl2, 1.2 MgSO4, 1 NaH2PO4, 10.0 glucose, and 26.0 NaHCO3] maintained at 30 ± 1˚C for at least 1 hr before recording. Slices were transferred to a recording chamber (Warner Instruments) submerged in normal, oxygenated aCSF and maintained at 28-30˚C at a flow rate of 2 ml/min. Tetrodotoxin (TTX) was included in the bath to prevent firing of action potentials and to allow accurate determination of changes in membrane potential. Neurons of the dorsal raphe were visualized using infrared- differential interference contrast (DIC) video-enhanced microscopy (Olympus). Slc6a4-positive cells labeled with hM3Dq-mCherry were identified using light from a mercury-vapor lamp filtered through a RFP filter cube. Borosilicate electrodes pulled with a Flaming-Brown micropipette puller (Sutter Instruments) with a pipette resistance between 3-6 MΩ filled with potassium gluconate solution [(in mM): 135 K+-gluconate, 5 NaCl, 2 MgCl2, 10 HEPES, 0.6 EGTA, 4 ATP, and 0.4 GTP, pH= 7.35, 290 mOsmol] were used to patch fluorescently-labeled cells in the dorsal raphe. Following establishment of a stable baseline membrane potential in current clamp mode, 10 μM CNO was bath applied for 10 min. The ability of CNO to depolarize cells was calculated by subtracting the baseline membrane potential from the average membrane potential over the last 2 min of CNO

application. Only cells with a stable access resistance (less than a 20% change from baseline to the end of the experiment) were used in the data analysis.

In Vivo Microdialysis. Mice were anesthetized with ketamine-xylazine as described above, and a guide cannula (CMA-7, CMA Microdialysis, Chelmsford, MA, USA) was stereotaxically implanted into the striatum (AP: 0.0 mm, ML: 2.2 mm, DV: 2.5 mm) relative to bregma. Operated mice were singly housed, given antibiotics in their drinking water for 48-72 hours (Pogorelov et al., 2005), and allowed to recover for 5-7 days. Mice were habituated to the microdialysis setting for 12 hours with food and water provided ad libitum before starting the experiment. Microdialysis probes (CMA-7, 2 mm membrane length, 0.24 mm o.d., Cuprophane, 6 K daltons cut-off; CMA Microdialysis, Chelmsford, MA, USA) were inserted into the guide cannula while gently restraining the animal and then perfused with artificial cerebrospinal fluid [(in mM): 147 NaCl, 2.7 KCl, 1.2 CaCl2, and 0.85 MgCl2] at 0.8 µl/min . After equilibrating for 3 hours, dialysates were collected for every 20 min and immediately frozen and stored at −80 °C until analysis. Samples were analyzed by high-performance liquid chromatography with electrochemical detection (HPLC-EC) using an Alexys monoamine analyzer (Antec, Palm Bay, FL, USA). The analyzer consisted of a DECADE II detector coupled to two C18 columns and two VT-03 flow cells (Antec). 5-HT was measured on a C18 reverse-phase 1 mm x 50 mm column with 3 µm particle size (ALF-105; Antec) using a mobile phase [50 mM phosphoric acid, 0.1 mM EDTA, 8 mM KCl, 12% MetOH, and 500 mg/l OSA, pH 6.0] and the potential set at 0.3 volts, while 5-HIAA was measured on another C18 reverse-phase 1 mm x 150 mm column with 3 µm particle size (ALF 115; Antec) with a mobile phase [50 mM phosphoric acid, 50 mM citric acid, 0.1 mM EDTA, 8 mM KCl, 10% MetOH, 500 mg/l OSA, pH 3.25] and the potential set at 0.62 volts.

The chromatograms were analyzed using the Clarity software package (DataApex, Prague, Czech Republic). The limit of detection was considered as a signal-to-noise ratio (SNR) of 3. The data collected over time were analyzed by repeated measures ANOVA (RMANOVA), while cumulative neurochemical levels were analyzed by t-tests; a $p < 0.05$ was considered significant.

Home Cage Monitoring (HCM) System. Data Collection. After 5 days of acclimation to the UCSF animal facility, mice were individually housed in 45 x 24 x 17 cm Plexiglas home-cage monitoring (HCM) enclosures. At one end of each enclosure was a photobeam-based feeding monitor and a capacitance-based lickometer. At the far end of the enclosure, across from the feeder was a 10 x 10 x 10 cm opaque black plastic housing niche with a cotton nestlet. The enclosures were mounted atop activity platforms providing animal location data at 20 msec intervals. A detailed description of HCM hardware has been reported (Goulding et al., 2008). Animals received ad libitum access to water by the lickometer and to a powdered version of the UCSF animal facility standard chow diet (PicoLab; Mouse Diet 20).

Experimental Schedule. For all animals (hM3Dq: n = 8, EGFP: n = 8), acclimation to the HCM cages and collection of baseline data occurred over a 15 day period. On Day 16 and for the remainder of the testing period, CNO was provided in the drinking water, at a concentration of 40 mg/L. Data collected during the 7-day periods (Days 8-15 and Days 22-29) were used for within-subject comparisons of behavioral patterns at baseline versus during CNO treatment, respectively. A detailed description of HCM behavioral data quality control procedures and analysis methods has been previously reported (Goulding et al., 2008). Following the CNO behavioral pattern collection period, we assessed the impact of DRN

serotonergic neuronal activation on exploratory behavior. We examined the responses of

CNO-treated Slc6a4-hM3Dq and Slc6a4-EGFP mice to a novel object placed within their

HCM cages. Four hrs prior to the dark cycle onset, a metal binder clip (2 inch wide, 1 inch

capacity; Officemate International) was affixed to the center of the long cage wall opposite

the housing niche for a period of 4 hrs.

HCM Measures. Data quality control methods for the detection and adjustment for

device errors were performed as described (Goulding et al., 2008). Standard HCM

assessment of ingestive behavior and movement patterns were performed as outlined

(Goulding et al., 2008). Briefly, we reported that mice are in two fundamental mutually

exclusive states: active states (ASs) and inactive states (ISs). ISs are characterized by

periods of low physical activity (including sleep and resting) occurring exclusively at the

nest. These alternate with ASs, during which bouts of feeding, drinking, locomotion and

other behaviors occur (Goulding et al., 2008). The regulation of AS properties are distinct

from those of bouts and are highly sensitive to circadian time (Goulding et al., 2008).

Exploratory responses to novel object presentation were assessed by analyzing locomotor

paths and determining the amount of time animals spent within a 7 cm radius of the object

during the first hour of exposure.

Behavior Studies. The following behavioral paradigms were initiated 45 min after

acute administration of CNO/vehicle or after 3-4 weeks of chronic administration of either

CNO/vehicle in the drinking water.

Locomotor Activity and Center Zone Time. Locomotor activity was assessed under

standardized environmental conditions in 40 x 40 x 30-cm Plexiglas chambers with a grid of

photo-beams spaced at 1.52 cm (VersaMax system; AccuScan Instruments, Columbus, OH)

as previously described (Abbas et al., 2009). Locomotor activity was recorded for 1 hr. Parameters measured included total distance traveled and time spent in the center zone of the chamber. Data was extracted using Fusion software (AccuScan Instruments, Columbus, OH).

Light-Dark Emergence Test. Light and dark preference was assessed under standardized environmental conditions in 40 x 40 x 30-cm Plexiglas chambers as described above, fit with a 16" L x 8" H x 5" W dark chamber on one side (VersaMax system; AccuScan Instruments, Columbus, OH). Light, dark, and doorway preferences were recorded for 10 min. Data was extracted using VersaMap software (AccuScan Instruments, Columbus, OH).

Forced Swim. Mice were individually placed into a Plexiglas cylinder (21 cm diameter, 28 cm height) containing 15 cm water (25 ± 0.5 °C) and were monitored for 6 min. Mobility, high mobility, and immobility bouts were analyzed using EthoVision XT7 for the last 4 mins of the test. After the swim session, mice were dried and placed in their home-cage surrounded by a cotton cloth. The water was changed between each animal. Animals that were unable to perform the task were not included in this study.

Novelty-Suppressed Feeding. Food was removed from the home-cage 24 hr before testing. Mice were weighed just before food deprivation and again before testing to assess body weight loss. For testing, mice were placed into a brightly lit open field ($40 \, cm \times 40 \, cm \times 30 \, cm$ white plastic boxes containing 2 cm of bedding) with a food pellet at the center. Latency to begin eating the food was recorded. The total amount of food consumed during a 5 min period after returning to the home-cage was measured to test whether feeding differences in the novel environment were due to differences in hunger/motivation. These studies were performed after the first 4 hrs of the light cycle.

DREADD-assisted metabolic mapping (DREAMM). Slc6a4-Cre mice expressing

hM3Dq (n=8) or EGFP (n=8) in the dorsal raphe Slc6a4 positive neurons were transported to

the μPET facility the day prior to each scan to ensure habituation to the transportation

procedure and environment. All mice were then fasted overnight to attain consistency in

blood glucose levels as abnormal blood glucose levels interfere with FDG uptake (Wong et

al.). The following morning mice received an injection (i.p.) of either vehicle or CNO (2

mg/kg). This occurred four times, twice before (acute-vehicle and acute-CNO) and twice

after 3 weeks of daily (5 mg/kg, p.o.) CNO exposure (chronic-vehicle and chronic CNO).

Therefore each mouse was scanned four times. For each acute and chronic phase, vehicle and

CNO scans were separated by two days. For acute phase scans, vehicle preceded CNO while

for chronic phase scans, CNO preceded the vehicle (for the purpose of minimizing

withdrawal effects due to disruption of daily CNO administration after chronic exposure).

Twenty min after vehicle or CNO injections mice received an injection (i.p.) of ~0.2 mCi of

[18F]fluorodeoxyglucose (FDG) and were immediately placed in an open-field arena (40.64

x 40.64 x 40.64 cm) coupled to an activity monitoring system (Truscan, Coulbourn

Instruments, Whitehall, PA). Thirty min later mice were anesthetized with 1.5% isoflurane,

placed in a prone position on the bed of an R4 microPET rodent scanner (Siemens Medical

Solutions, Malverne, PA) and scanned using a 20 min static acquisition protocol. Scanning

procedures, image processing, and analysis were performed as previously described

(Michaelides et al., 2013; Michaelides et al., 2010).

2.3. RESULTS

2.3.1. hM3Dq receptors selectively expressed in DRN serotonergic neurons increase membrane excitability and 5-HT release.

Selective expression of the hM3Dq receptor (Armbruster et al., 2007) in DRN serotonergic neurons was achieved through stereotaxic injection of a previously characterized Cre-recombinase-dependent adeno-associated virus (AAV; (Krashes et al., 2011)) into the dorsal raphe of Slc6a4-Cre mice (Fig. 3A). Immunofluorescence microscopy revealed that 96.7% ±1.6, (N= 3670 cells) of hM3Dq expressing neurons co-localized with 5-HT-positive neurons with a 64.2% ±5.3 (N= 3670 cells) transduction efficiency of DRN 5-HT-containing neurons (Fig. 3A,B). A similar degree of co-localization and transduction efficiencies were observed in Slc6a4-Cre mice stereotaxically injected with a control Cre-dependent, AAV-containing EGFP virus (97.7% ±1.2 co-localization, N= 2035 cells; 73.5% ±4.6 transduction efficiency, N= 2035 cells; Fig. 7A,B). In addition, 5-HT-positive axons emanating from the dorsal raphe co-localized with hM3Dq receptors, thus demonstrating the trafficking of the hM3Dq receptor to the DRN serotonergic axons (Fig. 7C). Importantly, there was negligible expression of hM3Dq in 5-HT-positive neurons of the medial raphe (hM3Dq: 2.3% ±3.0; N= 586 cells; Fig. 7D), thus further highlighting selective expression of hM3Dq in 5-HT-positive neurons in the DRN.

To assess how the activation of hM3Dq receptors affected the electrophysiological properties of these DRN serotonergic neurons, whole cell, current-clamp recordings were performed in hM3Dq and EGFP expressing-neurons. After CNO exposure, a significant increase in membrane potential was observed in hM3Dq-positive DRN neurons in Slc6a4-

hM3Dq mice compared to EGFP-positive DRN neurons in Slc6a4-EGFP mice (Fig. 3C,D).

Importantly, hM3Dq- and EGFP-containing neurons had similar resting membrane potentials

(Fig. 3E). In vivo microdialysis was utilized to measure CNO's effects on 5-HT and 5-

hydroxyindoacetic acid (5-HIAA) concentrations in the striatum (a major DRN projection).

A significant increase in both 5-HT and 5-HIAA concentrations in Slc6a4-hM3Dq mice

compared to Slc6a4-EGFP mice (Fig. 3F-I) was observed after CNO administration.

Importantly, the concentration of dopamine and its measured metabolites were not altered

following CNO administration (Fig. 8).

2.3.2. Stimulation of DRN serotonergic neurons alters feeding in a circadian-dependent manner.

We next utilized a quantitative, robust, and automated procedure to assess how the

activation of DRN serotonergic neurons alters home cage behavioral organization. We

examined behavioral patterns prior to (Days 8-15) and during the second week of continuous

CNO treatment (Days 22-29) in Slc6a4-EGFP and Slc6a4-hM3Dq mice. Although no

significant effects of CNO treatment on total daily food intake were observed in either group,

examination of light cycle (LC) and dark cycle (DC) food intake revealed a significant effect

in Slc6a4-hM3Dq mice (Fig. 4A and 9A). Whereas CNO suppressed DC food intake by 0.24

gm, CNO enhanced LC food intake by 0.26 gm (Fig. 4A). By contrast, CNO treatment

produced no significant changes in DC or LC food intake in EGFP mice (Fig. 9A).

Moreover, no differences in food intake patterns of Slc6a4-hM3Dq and Slc6a4-EGFP mice

were found prior to CNO treatment. For a more detailed assessment of the influence of CNO

on circadian patterns of feeding in Slc6a4-hM3Dq mice, we examined food intake in 2-hr

bins throughout the circadian cycle and observed significant effects at the circadian time (CT) 1 and 3 hr time points (Fig. 4B). These results indicate that DRN activation induced by CNO produced a suppression in DC food intake that was followed by an enhancement in LC food intake of similar magnitude, resulting in no net change in daily intake. Moreover, the CNO-induced increase in LC food intake occurred exclusively during the first 4 hours of the LC.

We previously demonstrated that circadian patterns of food consumption are determined by both active state (AS) regulation and feeding-bout regulation (Goulding et al., 2008). Specifically, food consumed during a particular time of day is dependent on the probability that animals are engaged in ASs, as well as in the numbers and sizes of feeding-bouts that occur during those ASs. Moreover, AS and feeding-bout properties can be differentially altered by perturbations of genes implicated in energy balance (Goulding et al., 2008). We therefore examined the relative contributions of AS and feeding-bout regulation on the feeding effects of CNO in Slc6a4-hM3Dq mice. Examination of AS probability (ASP) in Slc6a4-hM3Dq mice revealed circadian influences of CNO treatment that paralleled those seen on food intake (Fig. 4C). Although the average daily ASP was not affected by CNO, a significant reduction in DC ASP was observed, and this was found to be countered by a significant enhancement in LC ASP. Whereas CNO suppressed DC ASP, it enhanced LC ASP (Fig. 4C). This effect of CNO was not observed in Slc6a4-EGFP mice (Fig. 9B). For a more detailed assessment of the influence of CNO on circadian patterns of ASP in Slc6a4-hM3Dq mice, we examined the ASP occurring during 2-hr bins throughout the circadian cycle and observed significant effects at the CT 15, 1, and 3 hr time points (Fig.

4D). These results indicate that in Slc6a4-hM3Dq mice, CNO-induced circadian shifts in food intake are strongly mimicked by circadian shifts in ASP

We next determined the extent to which changes in feeding-bout number contributed to the shifts in the circadian pattern of feeding in CNO-treated Slc6a4-hM3Dq mice. We examined daily feeding-bout totals prior to (Days 8-15) and during the second week of CNO treatment (Days 22-29) in Slc6a4-EGFP and Slc6a4-hM3Dq mice. No significant effects of CNO treatment on daily feeding-bout totals were observed in either group. However, in accord with its effects on LC food intake and ASP, CNO treatment increased LC feeding bout numbers in Slc6a4-hM3Dq mice whereas no alterations were observed in Slc6a4-EGFP mice (Fig. 4E and 9C). For a more detailed assessment of the influence of CNO on circadian patterns of feeding-bout rates, we examined them during 2-hr bins throughout the day and revealed a significant effect at the CT1 and 3 hr time points (Fig. 4F). These results indicate that increased feeding bout rates contribute to the CNO-induced enhancement of feeding early in the light cycle in Slc6a4-hM3Dq mice.

We next determined the extent to which changes in feeding-bout size contributed to the shifts in the circadian pattern of feeding in CNO-treated Slc6a4-hM3Dq mice. We examined feeding-bout sizes prior to (Days 8-15) and during the second week of CNO treatment (Days 22-29) in Slc6a4-EGFP and Slc6a4-hM3Dq mice. No significant effects of drug treatment on daily, DC, or LC feeding-bout sizes were observed in either group (Fig. 4G and 9D). For a more detailed assessment of the influence of CNO on circadian patterns of feeding-bout size in Slc6a4-hM3Dq mice, we examined feeding bouts during 2-hr bins throughout the circadian cycle and revealed no significant effects of CNO treatment (Fig. 4H). These results indicate that changes in feeding bout size do not contribute substantially

to the CNO-induced enhancement of feeding in the first 4 hrs of the LC in Slc6a4-hM3Dq mice.

We had previously found that once ASs are initiated, a characteristic shift occurs in the probabilities of distinct behaviors as the AS progresses (Goulding et al., 2008). Notably, feeding is the predominant activity occurring during the first 2 min of ASs, after which feeding probabilities decline rapidly, in a manner presumably reflecting satiation (Goulding et al., 2008). We therefore examined the extent to which the increased food intake exhibited by Slc6a4-hM3Dq mice early in the LC is accompanied by changes in the temporal patterns of food intake within ASs. We examined ASs exhibited during the first 4 hrs of the LC on testing days prior to (Days 8-15) and during the second week of CNO administration (Days 22-29). We aligned the onsets of these ASs (Fig. 4J and K) and then determined, on a min-by-min basis from AS onset, the probabilities that animals engaged in feeding behavior (Fig. 4I). This analysis revealed significant effects at the 4, 5, 6, 7, and 10 min time-points (Fig. 4I).

2.3.3. Acute activation of DRN serotonergic neurons induces anxiogenic and anti-depressant drug-like behavioral responses and the recruitment of discrete brain circuits.

We next evaluated how acute activation of DRN serotonergic neurons might influence anxiety-like and antidepressant-like behaviors. We first assessed whether acute activation of DRN serotonergic neurons could alter anxiety by utilizing a light-dark emergence paradigm and center time measurements from an open field trial. As shown in Figure 5A, acute administration of CNO produces a minor, but statistically significant,

reduction of time spent in the lighted chamber and a reciprocal increase of time spent in the darkened chamber when comparing Slc6a4-hM3Dq mice to Slc6a4-EGFP control animals. Importantly, there was no difference in the number of entries into the darkened and lighted chambers when comparing Slc6a4-hM3Dq and Slc6a4-EGFP mice (Fig. 10B). Similar to the light-dark emergence test, the anxiogenic-like response after acute administration of CNO is also observed by monitoring center time in the open field when comparing Slc6a4-hM3Dq mice and Slc6a4-EGFP mice (Fig. 5B). Importantly, Slc6a4-hM3Dq and Slc6a4-EGFP mice have similar locomotion profiles after acute injection of CNO, suggesting that decreases in center time are not related to decreases in locomotion (Fig. 10A). The number of entries into the center of the open field revealed a decrease when comparing the Slc6a4-hM3Dq mice to Slc6a4-EGFP controls (Fig. 10C). An additional negative control (vehicle or absence of CNO) study was performed using these same behavioral assays, which failed to detect any differences between Slc6a4-hM3Dq and Slc6a4-EGFP mice (Fig. 10D-F). Furthermore, acute CNO treatment exerted no apparent effects in these behavioral paradigms when compared to vehicle in Slc6a4-EGFP control mice (Fig. 10G-I).

In an effort to map behavioral profiles associated with acute DRN serotonin neuron activation in the open-field to regional brain responses, we used DREADD-assisted metabolic mapping (DREAMM), which enables whole-brain circuit dissection in response to cell type-specific signaling manipulations in behaving rodents (Michaelides et al., 2013). Concurrent with a reduction in time spent in the center of the open field, DREAMM revealed that acute hM3Dq activation of DRN 5-HT neurons led to increased metabolic activity (i.e., FDG uptake) in the cingulate cortex (Cg2), the right inferior colliculus (IC), the right piriform (Pir), and primary somatosensory (SC), and motor cortices (MC) (Fig. 5D). In

39

contrast, decreases in FDG uptake were observed in the periaqueductal grey (PAG), anterior olfactory (AOM), and medial and central thalamic areas (MT and CT) (Fig. 5D). CNO was previously shown to not have any non-specific effects on FDG uptake (Michaelides et al., 2013). The specificity of DREAMM responses to the behaviors observed in the open field after acute hM3Dq activation were validated using both within-subject (scanned after vehicle-administered open field sessions) and between-subject controls (Slc6a4-EGFP mice), which did not show changes in time spent in the center of the open-field in response to acute DRN serotonin neuron activation.

Since acute administration of antidepressants can induce effects in some depression-related animal paradigms, we next evaluated whether acutely activating hM3Dq receptors in the DRN could induce antidepressant-like responses in the forced swim test (Porsolt et al., 1977). Following acute CNO administration, Slc6a4-hM3Dq displayed a significant reduction in immobility and a subsequent trend to an increase in mobility when compared to Slc6a4-EGFP control mice (Fig. 5C). As mentioned above, locomotion was not altered with this acute dose (Fig 10A). Hence, the decreased immobility cannot be attributed to an increase in general activity. Importantly, vehicle administration induced no significant alterations in mobility or immobility when comparing Slc6a4-hM3Dq and Slc6a4-EGFP mice (Fig. 10J). Finally, CNO demonstrated comparable immobility and mobility to vehicle in control mice (Fig. 10K).

2.3.4. Chronic activation of DRN serotonergic neurons induces an antidepressant-drug like effect.

Because SSRIs require many weeks of treatment before increases in mood and/or decreases in anxiety are observed, we next investigated the consequences of chronically activating DRN 5-HT neurons by combined behavioral and functional imagining analysis. We first determined if chronic administration of CNO could alter anxiety-like behaviors. After three weeks of CNO treatment, Slc6a4-hM3Dq and Slc6a4-EGFP mice spent a similar amount of time in the both the lightened and darkened chambers (Fig. 6A) as well as a similar center time in the open field (Fig. 6B). As a control the Slc6a4-hM3Dq and Slc6a4-EGFP mice entered a similar number of times in each of the three chambers of the light-dark exploration test and in the center zone of the open field (Fig. 11B and C). Chronic administration of CNO when compared to vehicle did not cause any significant changes in locomotion, time spent in the lightened or darkened chambers, or time spent in the center zone of the open field in Slc6a4-EGFP control mice (Fig. 11D-F).

Although no changes in anxiety-like behaviors were observed in these two behavioral paradigms, DREAMM revealed that chronic DRN 5-HT neuron activation produced widespread decreases in metabolic activity in many forebrain areas. Interestingly, a large reduction in FDG uptake was observed in hippocampal regions, specifically in CA1, the left dentate gyrus (DG), and the left dorsal subiculum (DS) (Fig. 6G and 12). Decreases in FDG uptake were also observed throughout most of the left habenula (Hb) along with areas of the left medial and central thalamic regions (MT and CT) (Fig. 6G and 12). In addition, FDG uptake was reduced in cortical areas including the left somatosensory cortex (SC), left primary motor cortex (MC), and left auditory cortex (AC) as well as hindbrain regions, such

as the medial parabrachial nucleus (MPB), dorsal and lateral dorsal tegmental (DTg and LDTg), the medial vestibular (MVe), and cerebellar nuclei (CBN) (Fig. 6G and 12). These widespread decreases in DREAMM responses were not observed in Slc6a4-EGFP control mice, which revealed no overlapping metabolic changes with CNO-exposed Slc6a4-hM3Dq mice. To investigate whether the continual activation of the hM3Dq receptor has led to the desensitization and/or down regulation of this receptor during chronic treatment, we used DREAMM again after an acute administration of CNO in chronically treated Slc6a4-hM3Dq mice. These scans revealed an intense increase in FDG uptake in the dorsal raphe area (Fig. 13) supporting the hypothesis that even following chronic activation, hM3Dq displays robust and continued activity.

To examine the effects of chronic CNO administration on the exploratory behaviors of Slc6a4-hM3Dq and Slc6a4-EGFP mice, a novel object was introduced into the home cage. Time spent by CNO-treated Slc6a4-hM3Dq and Slc6a4-EGFP mice within a 7 cm radius of the object (occupancy time) was analyzed over a 1 hr period following object placement. Time in the vicinity of the object was significantly enhanced in Slc6a4-hM3Dq, relative to Slc6a4-EGFP mice at the 20 minute time-point (Fig. 6E) and the patterns of exploratory interactions were also different (Fig 6F). Importantly, locomotor activities did not differ between the Slc6a4-hM3Dq mice and Slc6a4-EGFP control mice after chronic administration of CNO (Fig. 11A).

We next examined if chronic administration of CNO leads to antidepressant-like behavioral responses by utilizing the forced swim and the novelty-suppressed feeding tests. As shown in Figure 6C, a significant decrease in immobility and an increase in mobility were observed in Slc6a4-hM3Dq mice when compared to the Slc6a4-EGFP control mice,

42

demonstrating robust and prolonged antidepressant-like effects from chronic treatment with CNO. Importantly, compared to vehicle, the chronic administration of CNO did not alter immobility or mobility in control mice (Fig. 11G). Further characterization of this antidepressant-like phenotype resulting from chronic treatment was evaluated using the novelty-suppressed feeding paradigm, which is reported to be one of the few behavioral tests that is differentially sensitive to the chronic versus acute effects of antidepressant treatments (David et al., 2009; Santarelli et al., 2003). Chronic administration of CNO induced a large reduction in the latency to feed in Slc6a4-hM3Dq mice compared to Slc6a4-EGFP mice, while an acute dose of CNO showed no alteration in this behavior (Fig. 6D and 11H). Importantly, weight loss, initial body weight, and percentage of food consumed in the home cage after the testing were not different between Slc6a4-hM3Dq and Slc6a4-EGFP mice (Fig. 11I). Similarly, no significant alterations between mice were observed in these same parameters after vehicle administration (Fig. 11J). In addition, acute and chronic administration of CNO to control mice was also without effect when compared to vehicle (Fig. 11K-L). Taken together, these data provide further evidence that antidepressant-like behaviors can be induced by chronically activating hM3Dq receptors expressed in DRN 5-HT neurons.

CHAPTER 3. DISCUSSION AND FUTURE DIRECTIONS

3.1. DISCUSSION

Here we report that through chemogenetic manipulation we selectively activated the DRN 5-HT neurons and produced molecular, physiological, and behavioral effects that provide new insights into serotonergic regulation of neural pathways relevant to feeding, anxiety, and the mechanisms of antidepressant drug action. We also validated the hM3Dq chemogenetic technology extensively, showing via electrophysiological, neurochemical, and behavioral approaches that the effects of CNO correlated well with the selective activation of DRN 5-HT neurons after both acute and chronic stimulation. We demonstrated that selective DRN serotonergic activation increases neuronal membrane excitability as well as 5-HT release and turnover. Using a method that provides a quantitative characterization of behavioral organizations, we revealed changes in feeding patterns, shedding light on the serotonergic regulation of feeding, with implications for pharmacological approaches to obesity treatment. Furthermore, we discovered that both acute and chronic activation of DRN serotonergic neurons produces behavioral results resembling those of systemic SSRI administration. Additionally, we observed that acute and chronic activation of serotonergic neurons exerts widespread, but dramatically different, functional metabolic effects on network activity in mice which can be correlated with the differential effects on behavioral phenotypes.

Serotonin has long been considered as an anorectic agent, since treatments that globally enhance serotonergic neurotransmission generally suppress feeding behaviors; however the neural mechanisms underlying these actions are incompletely understood. This limitation is in part attributable to the multitude of regions throughout the neuraxis known to both modulate feeding and to receive serotonergic innervation. Of these regions, particular emphasis has been placed upon the medial hypothalamus, which is innervated by 5-HT neurons arising from the DRN (Willoughby and Blessing, 1987).

The application of a robust and sensitive quantitative behavioral analysis revealed a level of complexity in feeding responses mediated by DRN 5-HT neurons that has not been acknowledged in current models of serotonergic satiety. Although chronically stimulating serotonergic neurons in the DRN produced no net changes in daily food intake or body weight, it did alter circadian patterns of feeding. We detected a modest suppression of DC food intake that was precisely counterbalanced by an enhancement of LC food intake. These results are in accord with a prior report indicating that chronic infusion of 5-HT into the ventromedial hypothalamus of obsess Zucker rats diminished DC food intake while enhancing LC feeding (Fetissov and Meguid, 2010).

Previously, we described a hierarchical organization of behavioral regulation in which food intake levels at particular times of the day are determined by the properties of ASs and the feeding bouts occurring within ASs (Goulding et al., 2008). The regulation of AS and feeding-bout properties have been shown to be dissociable, raising the possibility that they involve distinct neural pathways. Here we find that the change in circadian feeding patterns produced by the activation of DRN 5-HT neurons occurs predominantly through modulation of AS properties. Specifically, CNO-induced changes in the circadian regulation

45

of AS probability closely mimicked changes in the circadian pattern of food intake. These increases in both LC food intake and LC AS probability occurred predominately during the first 4 hrs of the LC. By contrast, no changes in feeding-bout size were observed at this time.

Furthermore, we have previously found in C57BL/6 mice that, within individual ASs, the probability of feeding is highest within 2 min of AS onset, and that this probability subsequently declines rapidly over time (Goulding et al., 2008). This decline in feeding probability, which was dramatically suppressed in Lepob/ob mice, was proposed to reflect the process of satiation (Goulding et al., 2008). Here, CNO-treated Slc6a4-hM3Dq mice exhibit a blunted decline in AS feeding probability during the early LC, raising the possibility that the relative hyperphagia seen at this time is driven by a reduction in satiation. Altogether, these results reveal that a continuous selective 5-HT system manipulation can both decrease and increase food intake in a manner that is highly sensitive to circadian time. This demonstrates a level of complexity in serotonergic feeding regulation which contrasts with the common view that enhanced serotonergic neurotransmission uniformly suppresses feeding. These results indicate that a single 5-HT manipulation both can decrease and increase food intake in a manner that is highly sensitive to circadian time.

Selective control over serotonergic neuronal activity in the DRN enabled us to explore how acute and chronic hyper-serotonergic states modulate behavior and neuronal network activity. Acute stimulation of DRN serotonergic neurons induced an increase in anxiety-like behaviors; however these effects did not persist following 3 weeks of continuous activation. These data suggest a bi-phasic response in which initial increases in serotonergic activity from the dorsal raphe are anxiogenic, whereas chronic activation is without effect. Interestingly, after chronic treatment, a dramatic increase in the exploratory behavior of a

46

novel object was observed without any alterations in motor activity. This increase in exploratory behavior can be interpreted as a reduction in cautious and/or inhibitory behavior, a novel serotonergic-related behavioral effect, and it has correlations to various anxiolytic-related behaviors (Crawley, 1985).

Modulation of 5-HT levels has been strongly implicated in many therapies that alleviate depression (Kroenke et al., 2001). In addition, SSRI's have proven to be effective in various animal behavioral models that are utilized as preclinical screens (Willner, 1990). Selectively increasing DRN serotonergic neuronal activity revealed analogous antidepressant-like effects in several of these preclinical animal models. Thus acute stimulation of DRN serotonergic neurons produced an increase in the extracellular levels of 5-HT as well as a significant decrease in immobility and an increase in mobility in the classical antidepressant behavioral paradigm: forced swim. Chronic stimulation maintains this antidepressant-like activity, providing support for the notion that short- and long-term activation of the dorsal raphe serotonergic system plays an important role in mediating this behavioral response. A preclinical behavioral assay that better models the several week latency for clinical responsiveness to SSRIs is the novelty-suppressed feeding assay (David et al., 2009; Santarelli et al., 2003). In accord with these studies, chronic stimulation of the serotonergic neurons of the DRN in our model also reduces latencies to consume food in an aversive environment. Collectively, these data provide a strong case for implicating the involvement of this subset of serotonergic neurons in mediating antidepressant-like activity.

Mapping functional brain anatomy associated with acute and chronic hyper-serotonergic states in mice during behavior revealed alterations in regions that are implicated in anxiety and depression. Acute activation during the expression of an anxiogenic phenotype

in the open field highlighted a mix of changes in FDG uptake in anxiety-related and sensory processing nuclei. In particular, significant increases in functional metabolic uptake of FDG into the left cingulate and right piriform cortices was observed. Importantly, increased cerebral blood flow and glucose uptake in the cingulate cortex region has been strongly linked to anticipatory anxiety in humans (Chua et al., 1999; Javanmard et al., 1999; Straube et al., 2009) and anxiogenic contextual conditioning in rats (Luyten et al., 2012), while increases in FDG uptake in the piriform cortex appear after acute immobilization stress in rats (Sung et al., 2009). Of additional interest were the observed decreases in FDG uptake in the periaqueductal grey area during acute activation. While anxiety-like responses, such as freezing, are usually associated with an activation of these nuclei (Vianna et al., 2001), no previous studies have examined metabolic uptake in this brain region under acute hyper-serotonergic conditions. However, previous investigations have shown that direct 5-HT administration into this area by intra-cerebral injection results in an anxiogenic-like increase in avoidance (Zanoveli et al., 2003).

In contrast to acute stimulation, chronically activating serotonergic neurons in the DRN lead to widespread decreases in FDG uptake, specifically in the left dorsal and ventral hippocampal regions (CA1, DG, and DS), CA1 region of the right hippocampus, left habenula, medial and central thalamic regions as well as areas of the brain stem and cerebellum. Importantly, decreases in FDG metabolism in hippocampal regions have been observed in patients who respond to SSRI treatment (Kennedy et al., 2001; Mayberg et al., 2000; Seminowicz et al., 2004), further implicating the suppression of neuronal activity in this area to antidepressant efficacy. In addition to the hippocampus, decreased metabolism in the habenula region has also been linked to potential antidepressant actions (Shumake et al.,

2010). Evidence in support of this hypothesis has shown that hyper-activation of the habenula occurs during depressive mood symptoms induced by tryptophan depletion in humans (Roiser et al., 2009), as well as by increased excitatory synaptic activity on the lateral habenula in an animal model of learned helplessness (Li et al., 2011). Furthermore, 5-HT has been shown to suppress excitatory basal ganglia transmission onto the habenula, thereby blocking an aversive or anti-reward pathway (Shabel et al., 2012). The habenula has even been successfully targeted by deep brain stimulation (DBS) to suppress activity in a patient who failed to respond to antidepressant therapies (Sartorius et al., 2010), and there is currently an ongoing clinical trial using lateral habenula DBS for treatment-resistant depression (NCT01798407). Another metabolic alteration of interest is the decrease in FDG uptake in the thalamic nuclei observed in both the acute and chronic activation of the DRN serotonergic neurons. Patients who were administered SSRIs have also demonstrated decreases in glucose metabolism in the thalamic regions, although some of these studies indicate this observation occurs in both responders as well as nonresponders (Brody et al., 2001; Mayberg et al., 2000). These data demonstrate the pervasive consequences of selectively activating a relatively small group of serotonergic nuclei in the dorsal raphe, further elucidating how 5-HT can induce both anxiety-like activity as well as antidepressant-like responses by differentially modulating the same neurons.

In conclusion, our findings reveal that 5-HT systems regulate feeding in a complex manner that is highly sensitive to circadian time. These results have implications for serotonergic pharmacotherapies targeting obesity and metabolic disorders. Additionally, our data suggest that activation restricted to the DRN serotonergic neurons is sufficient to reproduce both acute and chronic effects of antidepressants that target 5-HT systems

globally. Finally we have been able to metabolically map the effects of selectively activating these neurons during behavior, revealing alterations in regions that are implicated in anxiety and depression. Beyond the insights into the serotonergic regulation of behavior provided by this work, it also highlights the power of DREADD-based chemogenetic strategies to dissect the functional consequences of both acute and chronic activation of complex neural pathways with an unprecedented level of precision.

3.2. FUTURE DIRECTIONS

While this study demonstrates the impact of selectively stimulating DRN serotonergic neurons, additional studies are required to further dissect and characterize the complex serotonin network. For example, the rostral raphe, making up 85% of the serotonergic neurons in the brain, can be broken down into two main subdivisions: the dorsal and the medial raphe, both of which send a majority of their projections into the forebrain. While their axons largely overlap, they innervate different regions of the brain and are further classified based on the types of axons they send out. The dorsal raphe's axons typically do not form chemical synapses and release serotonin through finely beaded varicosities, while the medial raphe form true chemical synapses. Given the differences between these two nuclei, which generate a vast majority of the CNS serotonin, differentially activating the two nuclei and examining the resultant effects on a variety of behaviors, such as feeding, anxiety, and antidepressant-like responses, combined with their influence on network activity, would yield a clearer picture of how each of these different nuclei contribute to the responses seen with SSRIs. Furthermore, manipulating the DRN and MRN serotonergic neurons in different mouse models of depression (for example: a stress induced model (Chaudhury et al., 2013)

50

and a serotonin deficient model (Jacobsen et al., 2012)), will further characterize the potential role of targeting these nuclei in relieving depression-like symptoms. Additionally, perturbing serotonin network dynamics by differentially silencing these two nuclei prior to examining behaviors that assess feeding, anxiety, and antidepressant-like responses would yield insight into how normal serotonergic tone influences these processes.

Studies aimed at gaining finer control of the serotonergic system can potentially reveal specific functions that can be assigned to different subdivisions of the dorsal raphe nucleus. This can be achieved through the use of DREADDs in combination with specific retrograded viruses such as AAV6 (Salegio et al., 2013). For example, gaining control of precise DRN serotonergic nuclei that project to specific areas (PBN, SCN, and various parts of the hypothalamus) potentially involved in the circadian dependent feeding alterations reported in this document will provide a more exact approach when examining serotonergic regulation of feeding behaviors. These same approaches can be applied to the cingulate cortex, amygdala and BNST projections from the DRN serotonergic neurons when interrogating serotonin's modulation of anxiety phenotypes. In general, most serotonergic projection areas can be targeted with this approach thus allowing for the control and characterization of different subgroups of serotonin neurons within the dorsal raphe and other serotonergic raphe nuclei. These future studies, utilizing more selective expression and fine-tune control of neurons, will further advance the dissection of this complex neurotransmitter network and contribute to our understanding of the serotonin system.

APPENDIX A. TABLES

Table 1. In Vivo DREADD Applications using Cre-Sensitive Viruses

This table is a quick reference for neuroscience research combining the DREADD technology and cell-type specificity achieved through Cre-sensitive viruses.

| Cell Type	Region	DREADD	In Vivo Response	Study
Orexin-containing neurons	Lateral Hypothalamus	hM3Dq / hM4Di	Increased wakefulness in hM3Dq infected mice; Decrease wakefulness in hM4Di infected mice	Sasaki, K. et al. 2011 PLoS One
AgRP-containing neurons	Arcuate Nucleus	hM3Dq / hM4Di	Increased food intake in hM3Dq infected mice; Decrease food intake in hM4Di infected mice	Krashes, M.J. et al. 2011 J. Clin. Invest.
AgRP-containing Neurons POMC-containing Neurons Sim1-containing Neurons	Arcuate Nucleus Paraventricular Hypothalamus	hM3Dq / hM4Di	Increased food intake in hM3Dq infected ArGP; Regulation of longterm food intake in hM4Di infected POMC; Stimulation of food intake with hM4Di infected Sim1	Atasoy, D. et al. 2012 Nature
RipII-containing Neurons	Arcuate Nucleus	hM3Dq	Increased energy expenditure and brown fat activity	Kong, D. et al. 2012 Cell
D1-containing Neurons D2-containing Neurons A2A-containing Neurons	Striatum	hM4Di	Changes in striatal excitatory synaptogenesis	Kozorovitskiy, Y. et al. 2012 Nature
MRGPRB4-containing Neurons	Sensory Neurons	hM3Dq	Induced Conditioned Place Preference	Vrontou, S. et al. 2013 Nature
Somatostatin-containing Neurons	Lateral Central Amygdala	hM4Di	Impairment of fear memory	Li, H. et al. 2013 Nat. Neurosci
Parvalbumin-containing Neurons	Binocular zone of the visual cortex	hM4Di	Extends the critical period for ocular dominance plasticity	Kuhlman, S. et al. 2013 Nature
GAD65-containing Neurons	Granule neurons of the horizontal limb of the diagonal band of Broca and magnocellular preoptic area	hM4Di	Impairment of the discrimination of structurally similar odors	Nunez-Parra, A. et al. 2013 PNAS
CAMKαII-containing Neurons	Orbital frontal cortex	hM4Di	Disrupts goal directed behavior	Gremel, C. et al. 2013 Nat. Commun.
POMC-containing Neurons	Arcuate Nucleus Nucleus tractus solitarius	hM3Dq	Inhibited feeding in ARC; Chronic treatment inhibited food intake in NTS	Zhan, C. et al. 2013 J. Neurosci
CGRP-containing Neurons	**Parabrachial Nucleus**	hM3Dq/ hM4Di	hM3Dq suppressed appetite; hM4Di increases food intake under anorexic conditions	Carter, M. et al. 2013 Nature

APPENDIX B. FIGURES
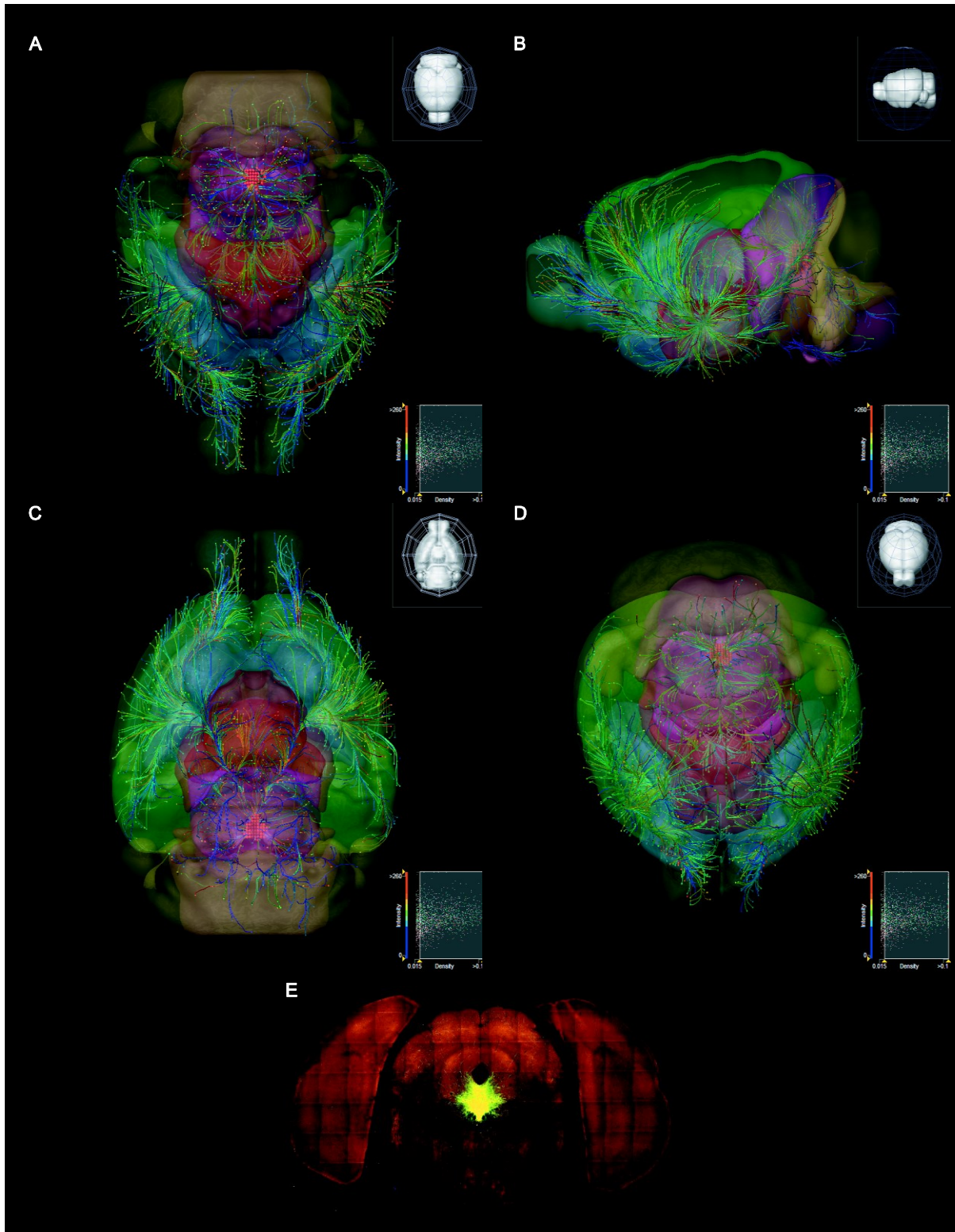
Figure 1. Dorsal raphe serotonergic neuronal projections

Rendered images obtained from the Allen Brain Connectivity Atlas (http://connectivity.brain-map.org/projection) in combination with Allen 3D Brain Atlas (http://connectivity.brain-map.org/static/brainexplorer). Anterograde labeling was generated by stereotaxically injecting 0.18 µl of rAAV2/1 pCAG-DIO-EGFP in the dorsal raphe of Slc6a4-Cre mice. Images for 3D rendering were obtained using a serial-two photon tomography technique. (A-D) Depicts all major brain regions (isocortex – light green, olfactory areas – blue, hippocampal formation – dark green, striatum – dark blue, thalamus and hypothalamus – red, midbrain – purple, medulla – light purple, pons – orange, and cerebellum – yellow) in different orientations (A – top, B – Side, C – Bottom, and D – Front) overlaid with the digital reconstruction of DRN serotonergic projections. (E) Coronal section demonstrating injection site of the Cre-sensitive EGFP expressing virus in the dorsal raphe.
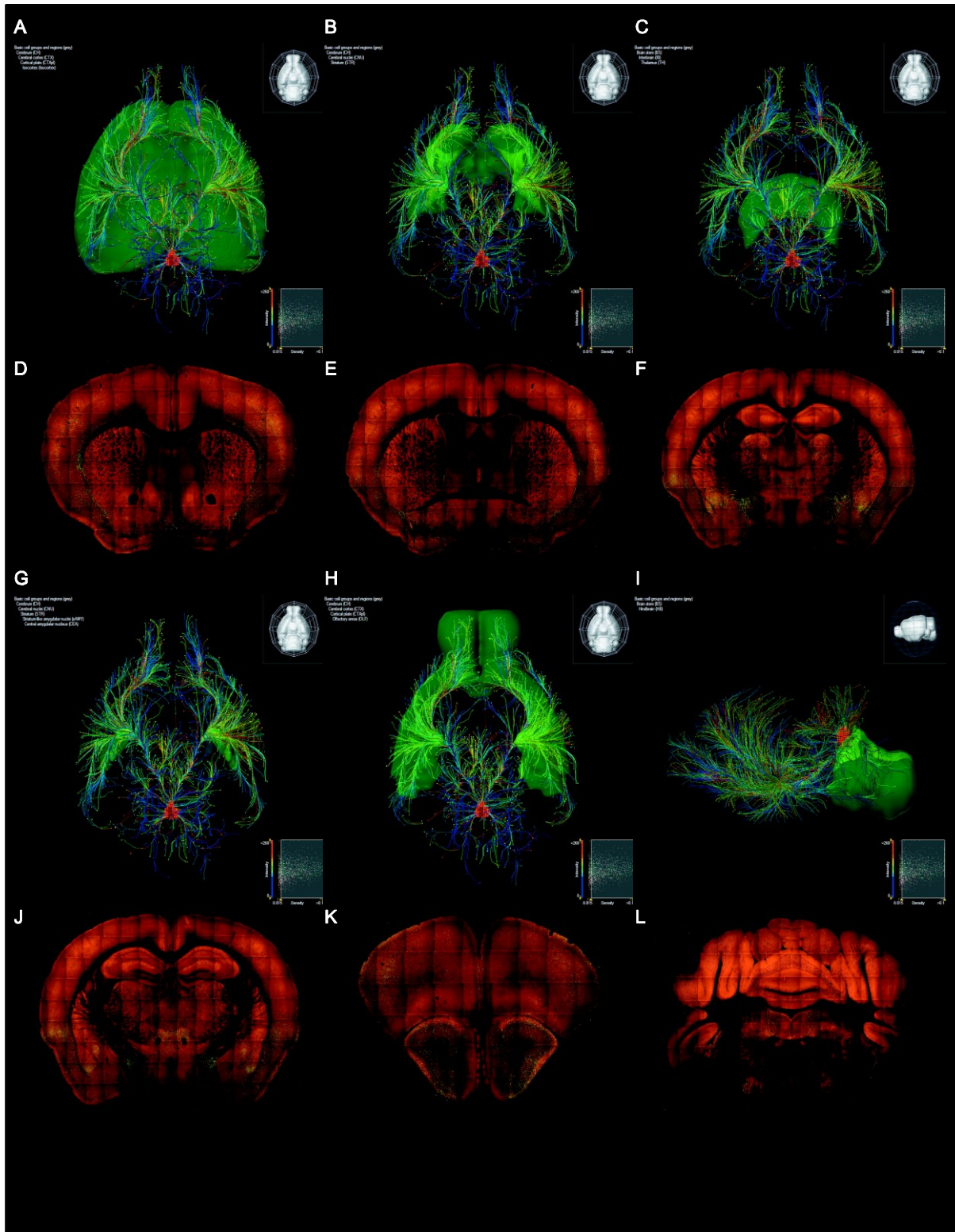
Figure 2. Dorsal raphe serotonergic projections highlighting the cerebral cortex, striatum, amygdala, thalamus, olfactory regions, and motor nuclei

Three dimensional rendering of the mouse brain overlaid with the digital reconstruction of DRN serotonergic projections highlighting the cerebral cortex (A), striatum (B), thalamus (C), amydgala (G), olfactory regions (H), and motor nuclei (I) shown in green. Coronal sections show Cre-sensitive EGFP expression in the cerebral cortex (D), striatum (E), thalamus (F), amydgala (J), olfactory regions (K), and motor nuclei (I).
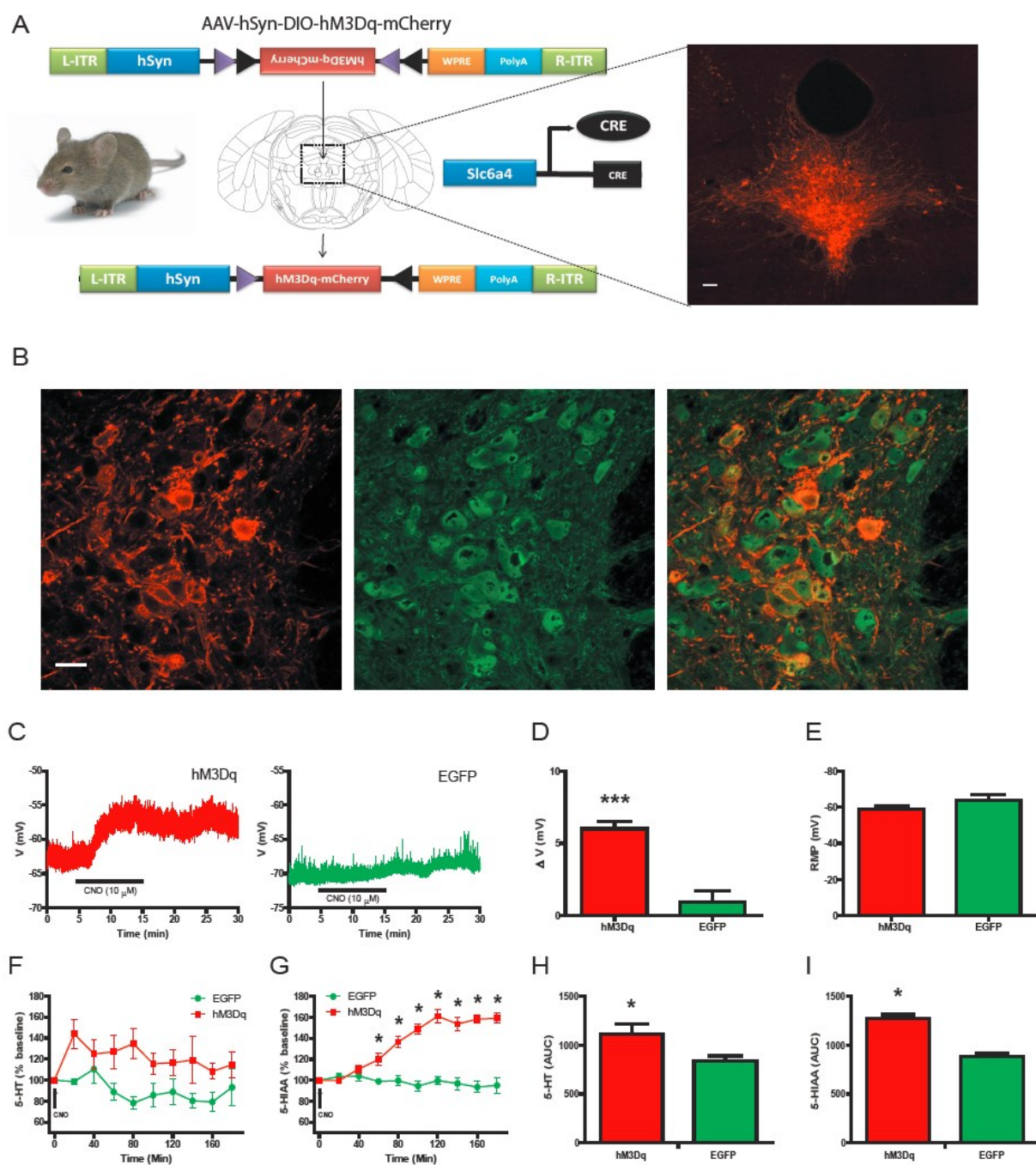
Figure 3. hM3Dq selectively expressed in DRN serotonergic neurons increases membrane excitability and 5-HT release upon activation

(A) Schematic demonstrating the design and stereotaxic injection of the Cre-sensitive hM3Dq-mCherry AAV driven off the human synapsin promoter. Right: mCherry fluorescence in the DRN after injections of the AAV-DIO-hM3Dq-mCherry virus into Slc6a4-Cre mice (scale: 200 µm). (B) Co-localization of mCherry (Red) and 5-HT (Green) in the DRN. The hM3Dq receptor is expressed in the plasma membrane while 5-HT is cytoplasmic (scale: 10 µm). (C) Whole cell, current clamp recordings from mCherry positive neurons from Slc6a4-hM3Dq mice and EGFP positive neurons from Slc6a4-EGFP control mice. (D) Change in membrane voltage in hM3Dq (N = 5) and EGFP (N=5) neurons after administration of CNO (unpaired t-test: * $p < 0.05$). (E) Resting membrane potential (RMP) from recorded hM3Dq and EGFP neurons. (F and G) Extracellular levels of 5-HT and 5-HIAA from the striatum of Slc6a4-hM3Dq (N=5) and Slc6a4-EGFP (N=6) mice determined by in vivo microdialysis after injection of CNO (RMANOVA: * $p < 0.05$). (H and I) Area under the curve (AUC) measurements for 5-HT and 5-HIAA (unpaired t-test: * $p < 0.05$).
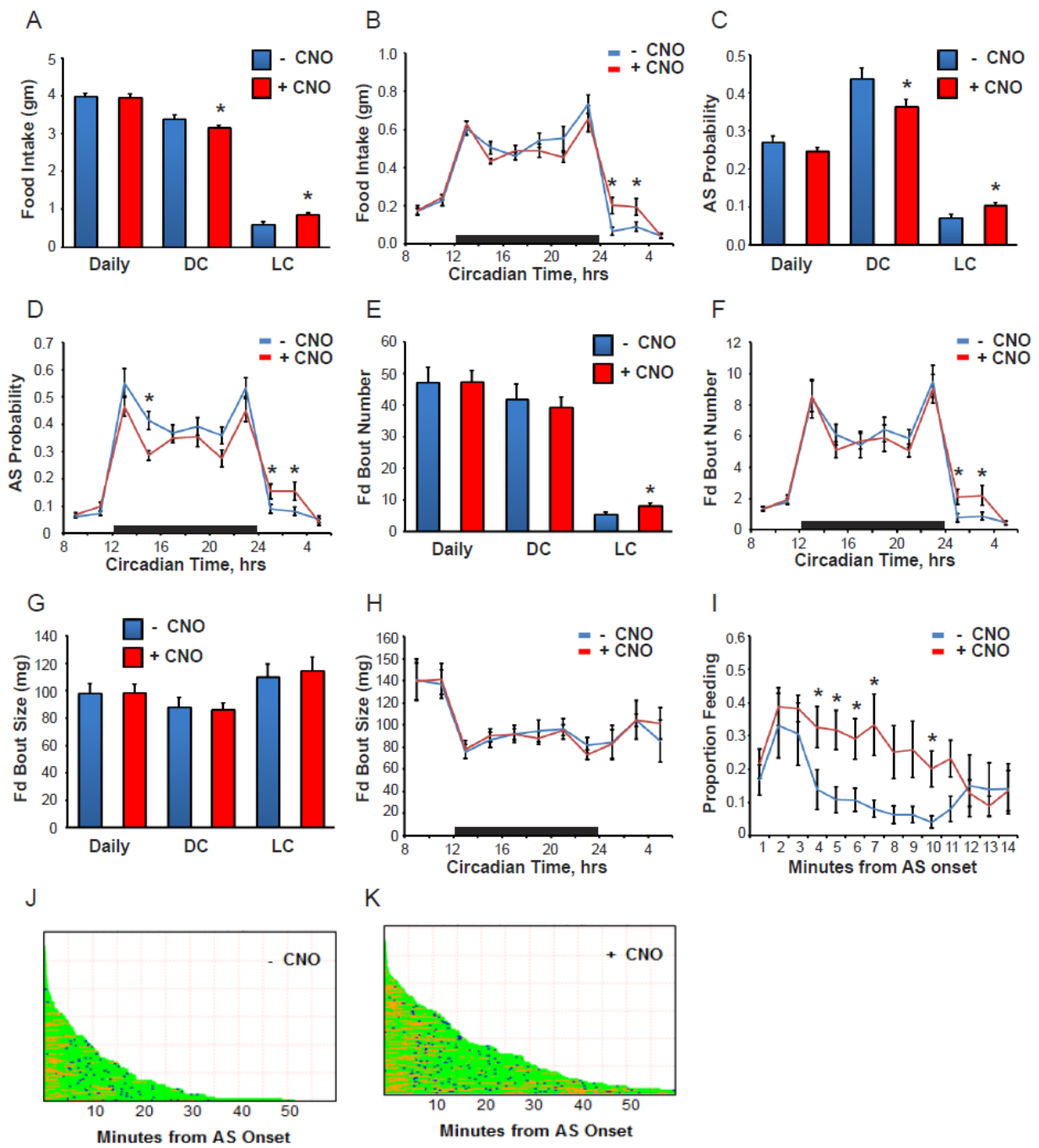
Figure 4. Activation of DRN serotonergic neurons alters feeding in a circadian-dependent manner

(A) Mean daily, dark cycle (DC) and light cycle (LC) food intake for Slc6a4-hM3Dq mice (N = 8) before and during CNO treatment (RMANOVA: * p < 0.05). (B) Mean food intake in 2-hr time bins for Slc6a4-hM3Dq mice (N = 8) before and during CNO treatment. Dark cycle indicated by black bar (RMANOVA: * p < 0.05). (C) Mean daily, dark cycle (DC) and light cycle (LC) active state probability for Slc6a4-hM3Dq mice (N = 8) before and during CNO treatment (RMANOVA: * p < 0.05). (D) Mean active state probability in 2-hr time bins for Slc6a4-hM3Dq mice (N = 8) before and during CNO treatment. Dark cycle indicated by black bar (RMANOVA: * p < 0.05). (E) Mean daily, dark cycle (DC) and light cycle (LC) feeding-bout number for Slc6a4-hM3Dq mice (N = 8) before and during CNO treatment (RMANOVA: * p < 0.05). (F) Mean feeding-bout number in 2-hr time bins for Slc6a4-hM3Dq mice (N = 8) before and during CNO treatment. Dark cycle indicated by black bar (RMANOVA: * p < 0.05). (G) Mean daily, dark cycle (DC) and light cycle (LC) feeding-bout size for Slc6a4-hM3Dq mice (N = 8) before and during CNO treatment. (H) Mean feeding-bout size in 2-hr time bins for Slc6a4-hM3Dq mice (N = 8) before and during CNO treatment. Dark cycle indicated by black bar. (I-J) Active states occurring during the first 4 hours of the light cycle for Slc6a4-hM3Dq (N = 8) mice, aligned by onset time prior to (I) and during (J) CNO treatment. Each row indicates an individual active state, in order (top to bottom) of increasing duration. Locomotor, feeding and drinking behavior indicated in green, orange and blue, respectively. (K) Feeding probabilities determined for 1-min time-bins, from time of active state initiation for Slc6a4-hM3Dq mice (N = 8) before and during CNO treatment (RMANOVA: * p < 0.05).
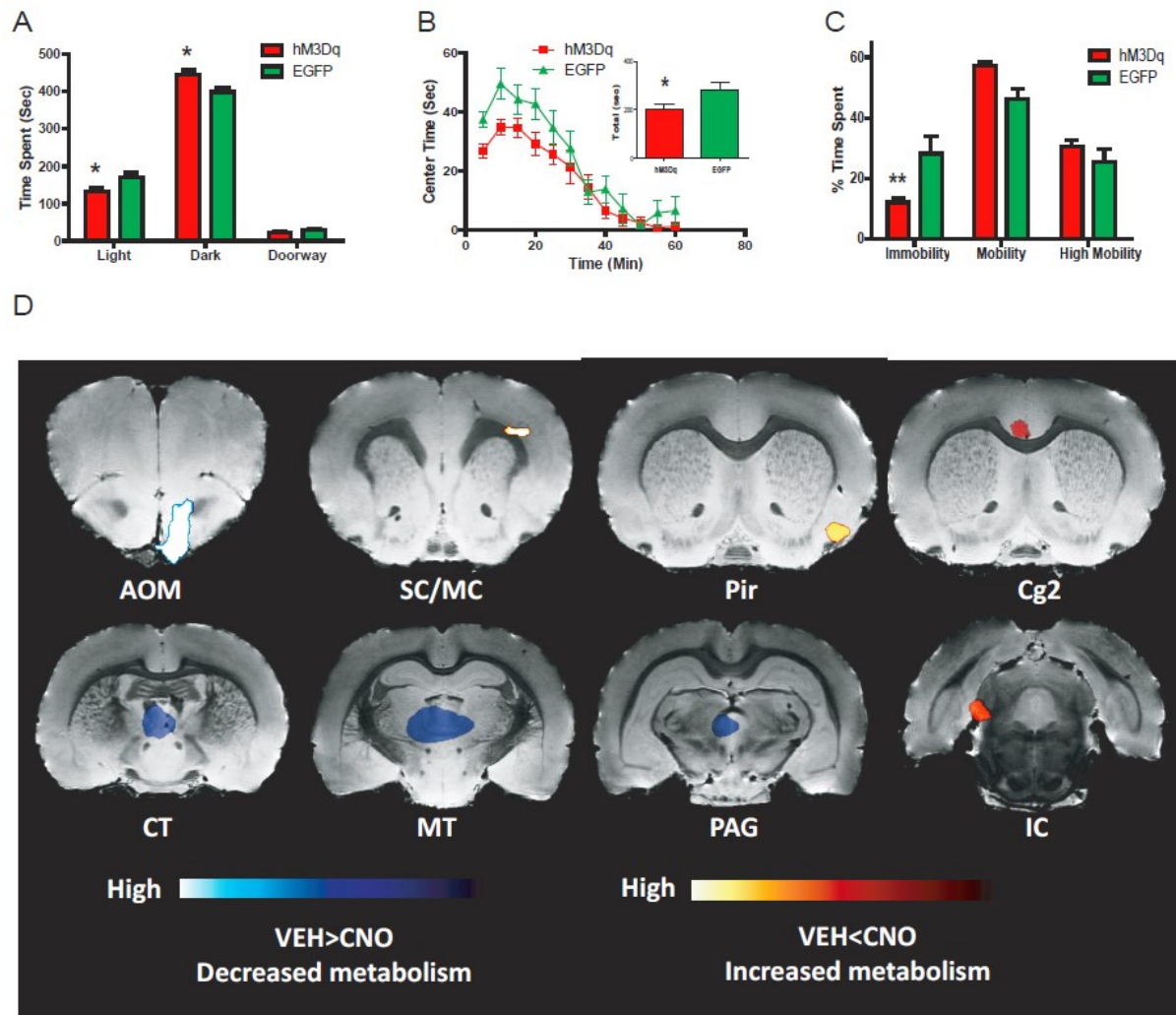
Figure 5. Acute stimulation of DRN serotonergic neurons induces anxiogenic- and antidepressant-like behavioral responses as well as modulation of neuronal circuits

(A) Time spent in the lighted, darkened, or doorway compartments by Slc6a4-hM3Dq (N = 15) and Slc6a4-EGFP (N = 13) mice over a 10-min period following acute administration of CNO (RMANOVA: * $p < 0.05$). (B) Time spent in the center of an open field by Slc6a4-hM3Dq (N = 16) and Slc6a4-EGFP (N = 16) mice shown in 5-min binned intervals after acute CNO administration (RMANOVA: between group difference * $p <$

0.05). Inset: Total center time for the 60-min trial (unpaired t-test: * $p < 0.05$). (C) Percent of time Slc6a4-hM3Dq (N = 9) and Slc6a4-EGFP (N = 9) mice exhibited immobility, mobility, and high mobility during the last 4-min of the forced swim test after acute injection of CNO (RMANOVA: * $p < 0.05$). (D) DREAMM responses after acute injection of CNO combined with an open-field exposure (p=0.05, relative increase (red) and decrease (blue) in FDG uptake; N=8, comparison of vehicle vs. CNO scans: within-subject comparison) Abbreviations: AOM – anterior olfactory nucleus (medial part), SC – primary somatosensory cortex, MC - primary motor cortex, Pir – piriform cortex, Cg2 – cingulate cortex 2, CT – central thalamic nucleus, MT – medial thalamic nucleus, PAG – periaqueductal grey, IC – inferior colliculus.
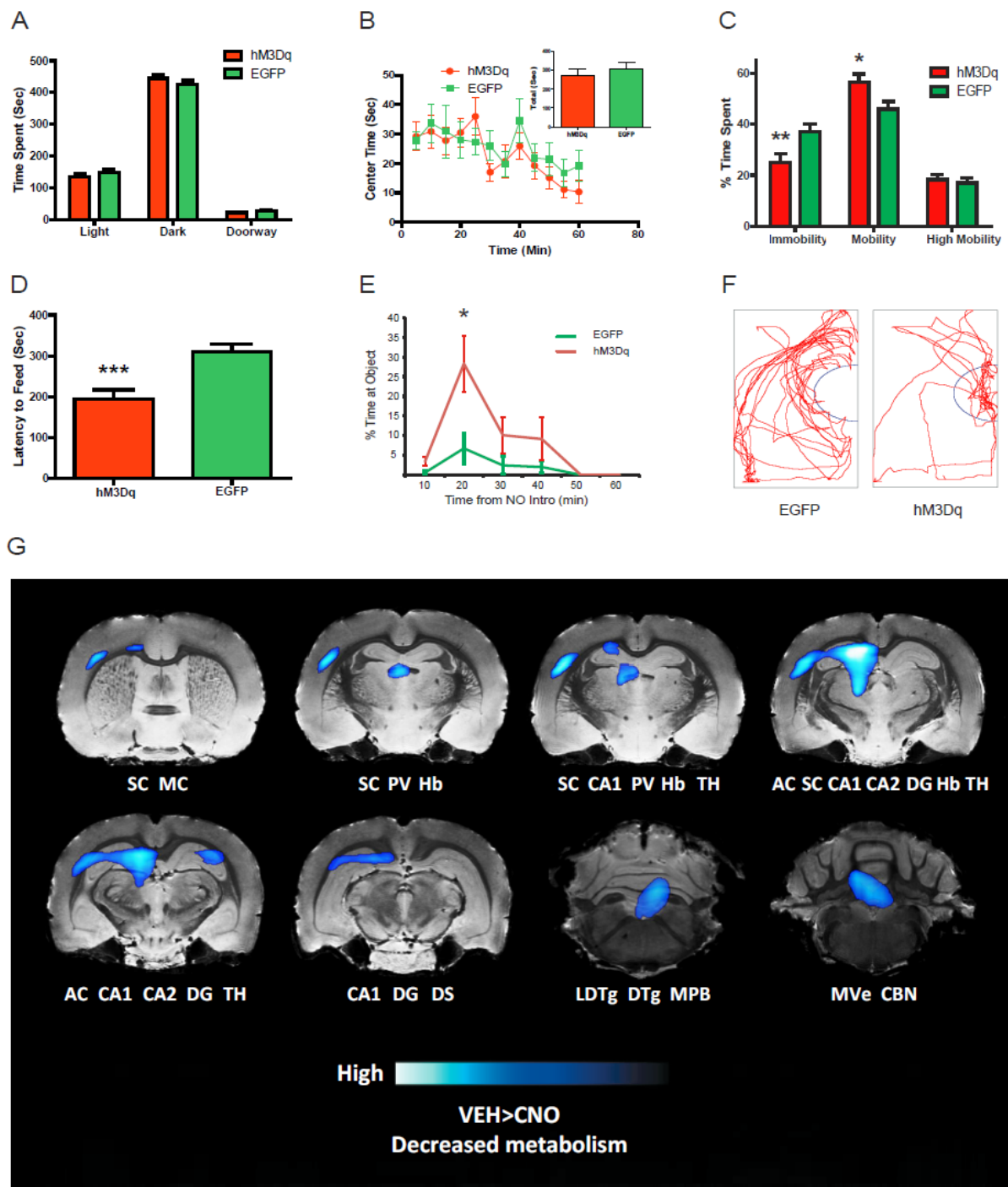
Figure 6. Chronic stimulation of the DRN serotonergic neurons produces antidepressant-like effects, increases exploration of a novel object, and suppresses neuronal circuits

(A) Time spent in the lighted, darkened, or doorway compartments by Slc6a4-hM3Dq (N = 17) and Slc6a4-EGFP (N = 17) mice over a 10-min period following chronic administration of CNO. (B) Time spent in the center zone of an open field by Slc6a4-hM3Dq (N = 17) and Slc6a4-EGFP (N = 17) mice in 5-min binned intervals after chronic administration of CNO. Inset: Cumulative center time over the 60-min test. (C) Percent of time Slc6a4-hM3Dq (N = 13) and Slc6a4-EGFP (N = 13) mice engaged in immobility, mobility, and high mobility during the last 4-min of the forced swim test after chronic administration of CNO (RTWANOVA: * $p < 0.05$). (D) Latency to feed by Slc6a4-hM3Dq (N = 17) and Slc6a4-EGFP (N = 17) mice after chronic administration of CNO in an aversive environment following food deprivation (unpaired t-test: * $p < 0.05$). (E) Percentage of time spent by Slc6a4-hM3Dq (N = 8) and Slc6a4-EGFP (N = 8) mice in vicinity of novel object during CNO treatment (RMANOVA: * $p < 0.05$). (F) Representative locomotor paths occurring 10-20 min after novel object placement, for Slc6a4-hM3Dq and Slc6a4-EGFP mice; the vicinity of the novel object indicated by blue hemicircle (7 cm radius). (G) DREAMM responses after chronic treatment of CNO combined with an open-field test (p=0.001, relative decrease (blue) in FDG uptake; N = 8, comparison of vehicle vs. chronic CNO scans: within-subject comparison) Abbreviations: SC – primary somatosensory cortex, MC - primary motor cortex, PV – paraventricular nucleus of the thalamus, Hb – habenula, TH – thalamus, DG – dentate gyrus, AC – auditory cortex, DS – dorsal subiculum, LDTg – lateral dorsal tegmental nucleus, DTg – dorsal tegmental nucleus, MPB – medial parabrachial nucleus, MVe – medial vestibular nucleus, CBN – cerebellar nuclei, and CA1 and CA2 – areas of hippocampus.
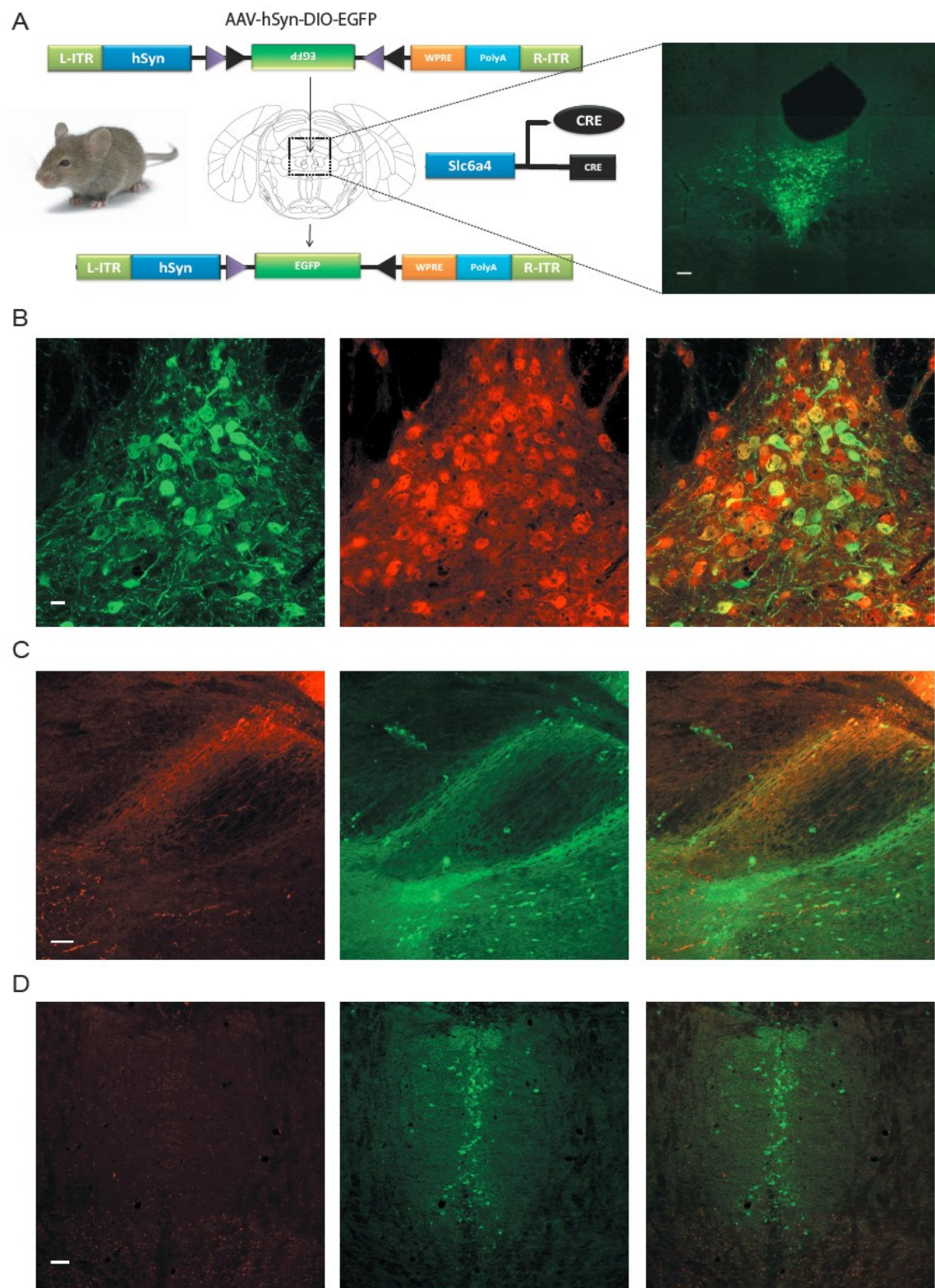
A

AAV-hSyn-DIO-EGFP

L-ITR | hSyn | EGFP | WPRE | PolyA | R-ITR

Slc6a4 — CRE

L-ITR | hSyn | EGFP | WPRE | PolyA | R-ITR

B

C

D

67

Figure 7. Selective expression of Cre-sensitive AAV in the DRN of Slc6a4-Cre mice

(A) Schematic demonstrating the design and stereotaxic injection of the Cre-sensitive EGFP control AAV driven off the human synapsin promoter. Right: EGFP fluorescence in the DRN after injections of the AAV-DIO-EGFP virus into Slc6a4-Cre mice (scale: 200 µm). (B) Co-localization of GFP (Green) and 5-HT (Red) in the DRN (scale: 10 µm). (C) Co-localization of hM3Dq receptor (Red) with 5-HT positive axons (Green) projecting from the DRN (top right) (scale: 50 µm). (D) Lack of co-localization of hM3Dq receptor (Red) with 5-HT positive neurons (Green) in the medial raphe nucleus (scale: 50 µm).
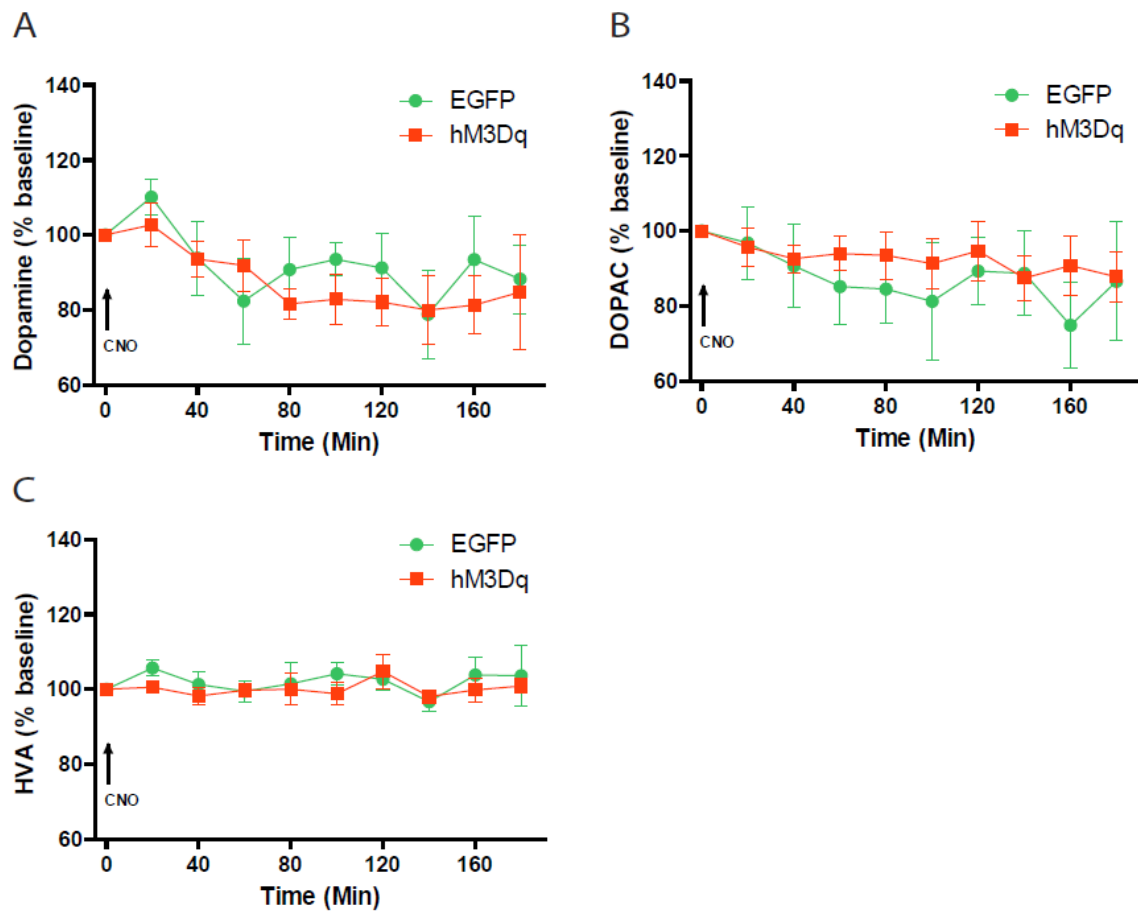
Figure 8. Extracellular dopamine and measured metabolites

Extracellular levels of (A) dopamine, (B) 3,4-dihydroxyphenylacetic acid (DOPAC),

and (C) homovanillic acid (HVA) from the striatum of Slc6a4-hM3Dq (N=5) and Slc6a4-

EGFP (N=6) mice determined by in vivo microdialysis after injection of CNO.
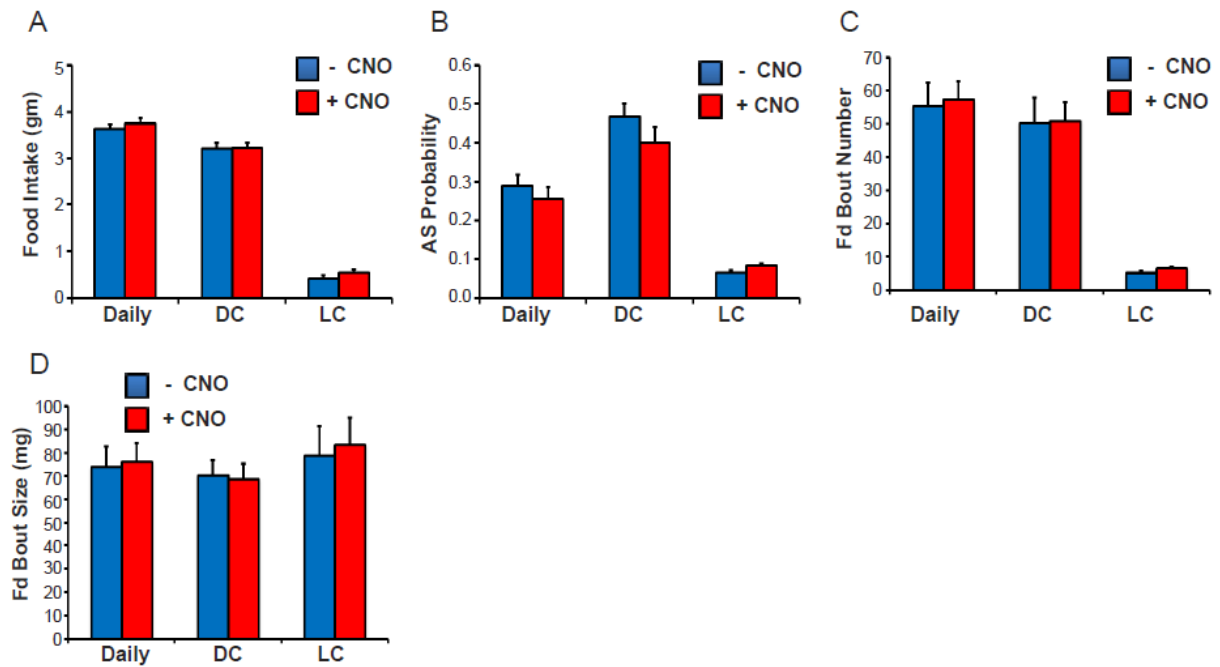
Figure 9. Administration of CNO does not alter feeding behaviors in Slc6a4-EGFP mice

(A) Mean daily, dark cycle (DC) and light cycle (LC) food intake for Slc6a4-EGFP mice (N = 8) before and during CNO treatment. (B) Mean daily, dark cycle (DC) and light cycle (LC) active state probability for Slc6a4-EGFP mice (N = 8) before and during CNO treatment. (C) Mean daily, dark cycle (DC) and light cycle (LC) feeding-bout number for Slc6a4-EGFP mice (N = 8) before and during CNO treatment. (D) Mean daily, dark cycle (DC) and light cycle (LC) feeding-bout size for Slc6a4-EGFP mice (N = 8) before and during CNO treatment.
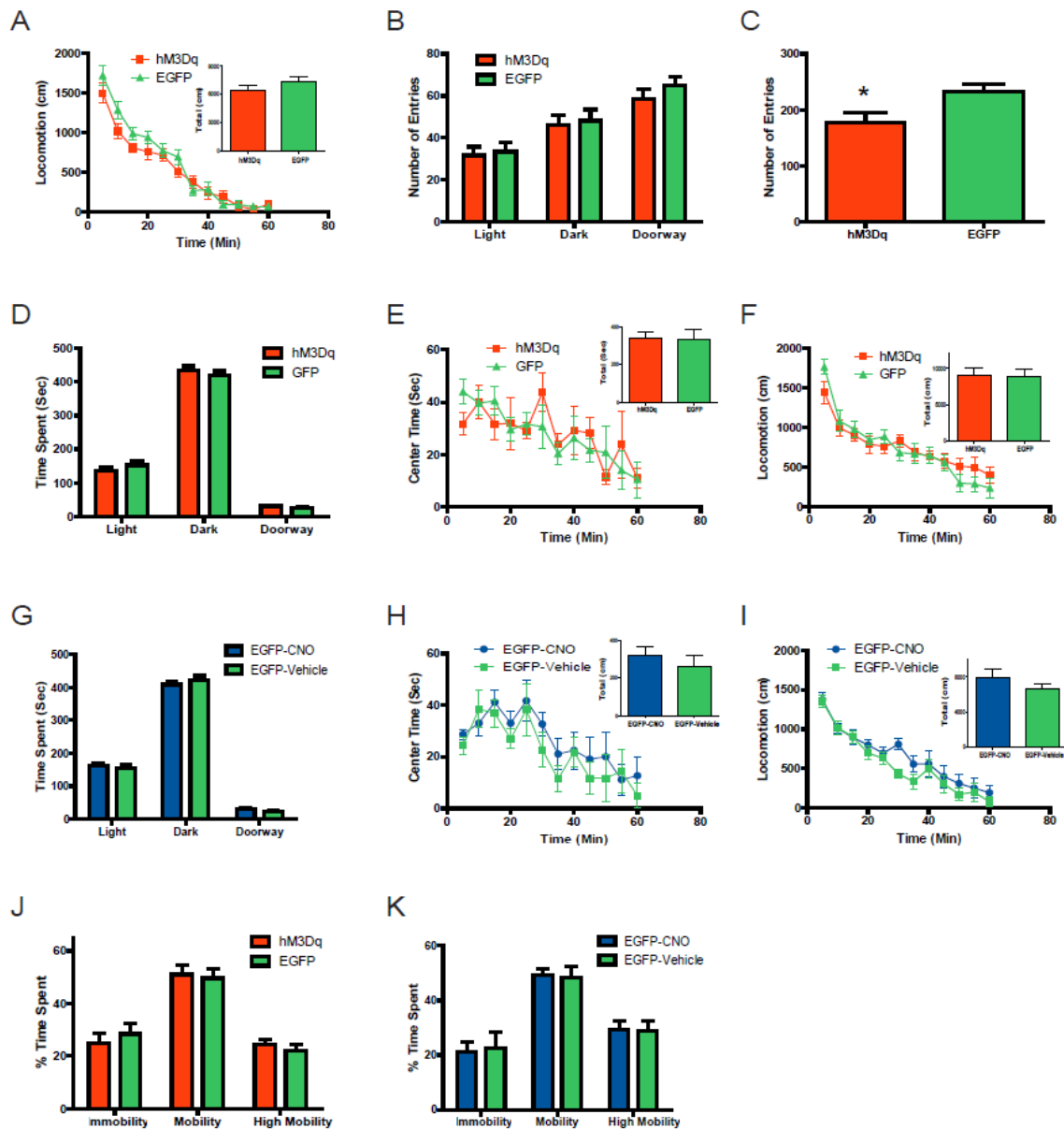
Figure 10. Behavioral control studies conducted following acute administration of CNO or vehicle

(A) Locomotor activities in Slc6a4-hM3Dq (N = 16) and Slc6a4-EGFP (N = 16) mice

in 5-min binned intervals following acute CNO administration. Inset: Cumulative distance

traveled (cm) over the 60-min test. (B) Number of entries into each chamber by Slc6a4-hM3Dq (N = 15) and Slc6a4-EGFP (N = 13) mice recorded during the 10-min light-dark test following acute administration of CNO. (C) Cumulative number of total entries into the center zone of the open field over 60 min by Slc6a4-hM3Dq (N = 16) and Slc6a4-EGFP (N = 16) mice recorded following acute CNO administration (unpaired t-test: * $p < 0.05$). (D) Time spent in the lighted, darkened, or doorway compartments by Slc6a4-hM3Dq (N = 8) and Slc6a4-EGFP (N = 8) mice over a 10-min period following acute administration of vehicle. (E) Time spent in the center of an open field by Slc6a4-hM3Dq (N = 8) and Slc6a4-EGFP (N = 8) mice in 5-min binned intervals after acute vehicle administration. Inset: Cumulative center time for the 60-min test. (F) Locomotor responses by Slc6a4-hM3Dq (N = 8) and Slc6a4-EGFP (N = 8) mice in 5-min binned intervals following acute vehicle administration. Inset: Cumulative locomotion (cm) over the 60-min test. (G) Time spent in the lighted, darkened, or doorway compartments by Slc6a4-EGFP mice over a 10-min period following acute administration of either CNO (N = 8) or vehicle (N = 8). (H) Time spent in the center of an open field by Slc6a4-EGFP mice in 5-min binned intervals after acute administration of either CNO (N = 8) or vehicle (N=7). Inset: Cumulative center time over the 60-min test. (I) Locomotor responses by Slc6a4-EGFP mice in 5-min binned intervals following acute administration of either CNO (N = 8) or vehicle (N = 7). Inset: Cumulative locomotion (cm) over the 60-min test. (J) Percent of time Slc6a4-hM3Dq (N = 9) and Slc6a4-EGFP (N = 9) mice exhibited immobility, mobility, and high mobility during the last 4-min of the forced swim test after acute administration of vehicle. (K) Percent of time Slc6a4-EGFP mice exhibited immobility, mobility, and high mobility during the last 4-min of the forced swim test after acute administration of either CNO (N = 8) or vehicle (N = 8).
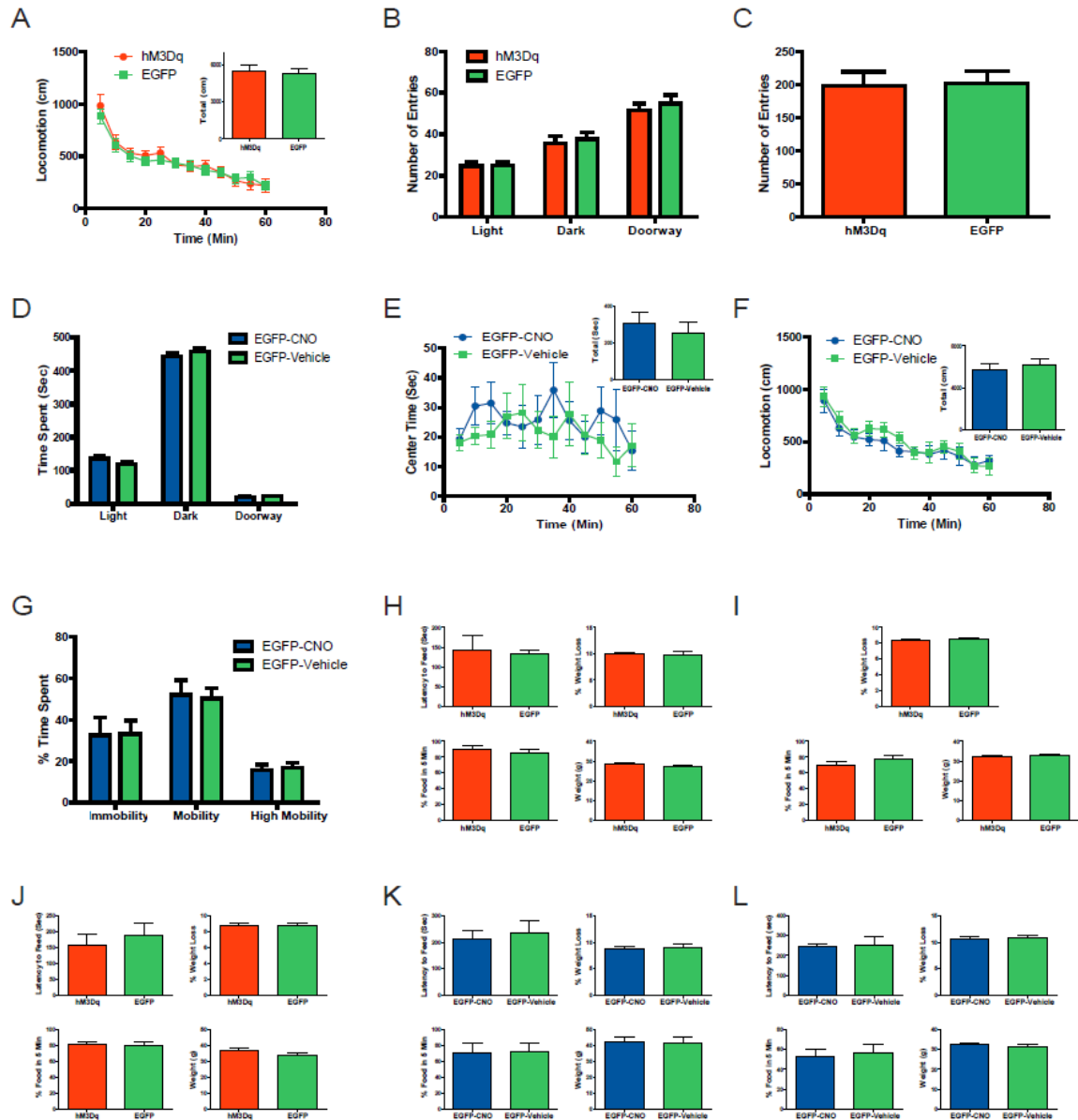
Figure 11. Behavioral control studies for chronic administration of CNO or vehicle and control studies for the novelty-suppressed feeding paradigm

(A) Locomotor responses by Slc6a4-hM3Dq (N = 17) and Slc6a4-EGFP (N = 17)

mice in 5-min binned intervals following chronic CNO administration. Inset: Cumulative locomotion (cm) over the 60-min test. (B) Number of entries into each chamber by Slc6a4-hM3Dq (N = 17) and Slc6a4-EGFP (N = 17) mice recorded during the 10-min light-dark test following chronic administration of CNO. (C) Cumulative number of entries into the center zone of the open field by Slc6a4-hM3Dq (N = 17) and Slc6a4-EGFP (N = 17) mice during the 60-min test following chronic CNO administration. (D) Time spent in the lighted, darkened, or doorway compartments by Slc6a4-EGFP mice over a 10-min period following chronic administration of either CNO (N = 8) or vehicle (N = 8). (E) Time spent in the center of an open field by Slc6a4-EGFP mice in 5-min binned intervals after chronic administration of either CNO (N = 9) or vehicle (N=9). Inset: Cumulative center time over the 60-min test. (F) Locomotor responses by Slc6a4-EGFP mice in 5-min binned intervals following chronic administration of either CNO (N = 9) or vehicle (N = 9) Inset: Cumulative locomotion (cm) over the 60-min test. (G) Percent of time Slc6a4-EGFP mice exhibited immobility, mobility, and high mobility during the last 4-min of the forced swim test after chronic administration of either CNO (N = 9) or vehicle (N = 10). (H) Latency to feed (top left), percent weight loss (top right), percent food consumed (5-min) in the home cage (bottom left), and starting weight before food deprivation (bottom right) from Slc6a4-hM3Dq (N = 8) and Slc6a4-EGFP (N = 8) mice after acute administration of CNO. (I) Percent weight loss (top), percent food consumed (5-min) in the home cage (bottom left) and starting weight before food deprivation (bottom right) from Slc6a4-hM3Dq (N = 17) and Slc6a4-EGFP (N = 17) mice after chronic administration of CNO. (J) Latency to feed (top left), percent weight loss (top right), percent food consumed (5-min) in the home cage (bottom left) and starting weight before food deprivation (bottom right) from Slc6a4-hM3Dq (N = 8) and Slc6a4-EGFP (N =

8) mice after acute administration of vehicle. (K) Latency to feed (top left), percent weight loss (top right), percent food consumed (5-min) in the home cage (bottom left) and starting weight before food deprivation (bottom right) from Slc6a4-EGFP mice after acute administration of either CNO (N = 5) or vehicle (N = 5). (L) Latency to feed (top left), percent weight loss (top right), percent food consumed (5-min) in the home cage (bottom left) and starting weight before food deprivation (bottom right) from Slc6a4-EGFP mice after chronic administration of either CNO (N = 9) or vehicle (N = 9).
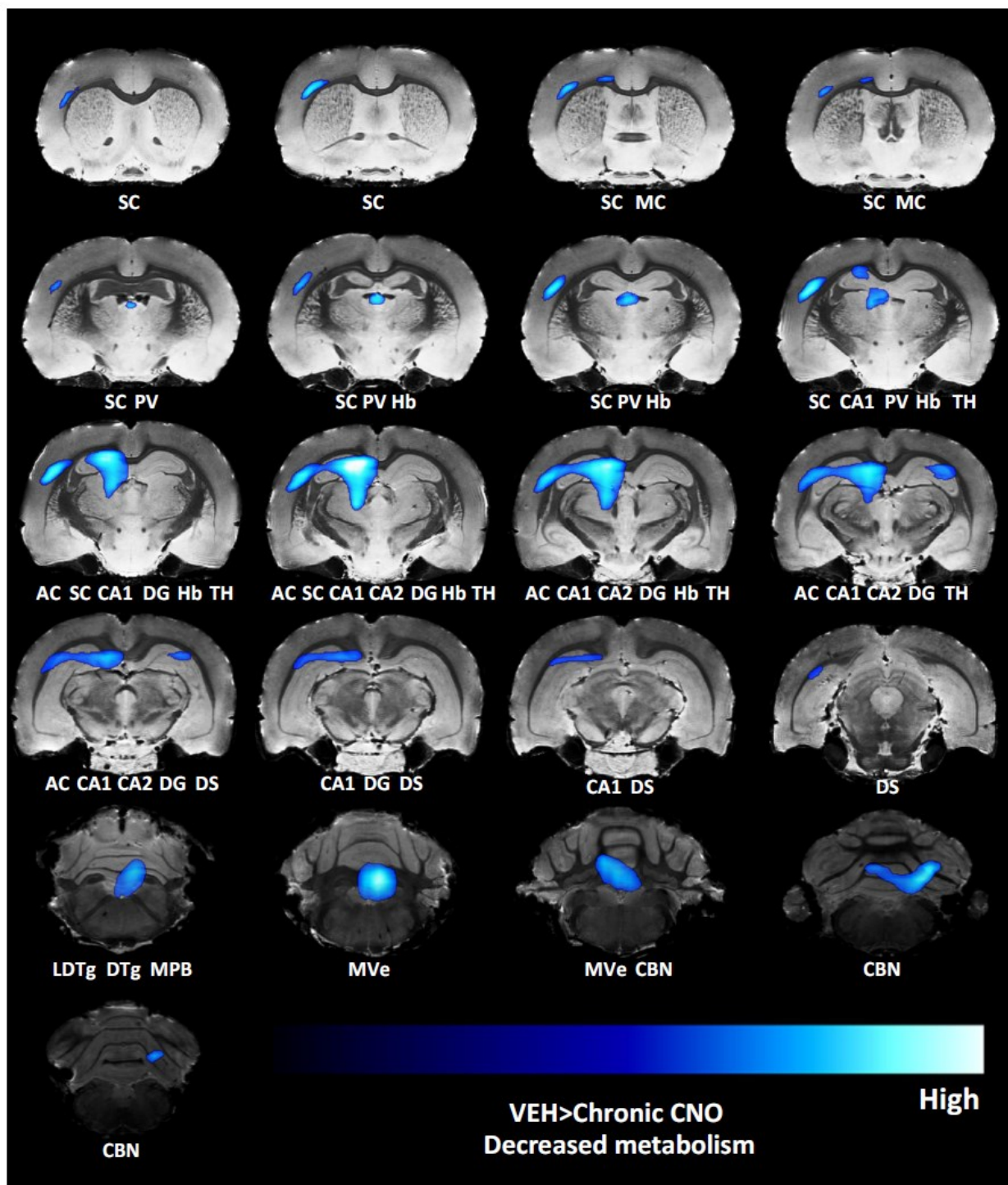
Figure 12. Complete DREAMM responses after chronic CNO treatment

Complete DREAMM responses after chronic CNO treatment combined with an open-

field test (p=0.001, relative decrease (blue) in FDG uptake; N = 8, comparison of vehicle versus chronic CNO scans: within-subject comparison) Abbreviations: SC – primary somatosensory cortex, MC - primary motor cortex, PV – paraventricular nucleus of the thalamus, Hb – habenula, TH – thalamus, DG – dentate gyrus, AC – auditory cortex, DS – dorsal subiculum, LDTg – lateral dorsal tegmental nucleus, DTg – dorsal tegmental nucleus, MPB – medial parabrachial nucleus, MVe – medial vestibular nucleus, CBN – cerebellar nuclei, and CA1 and CA2 – areas of hippocampus.
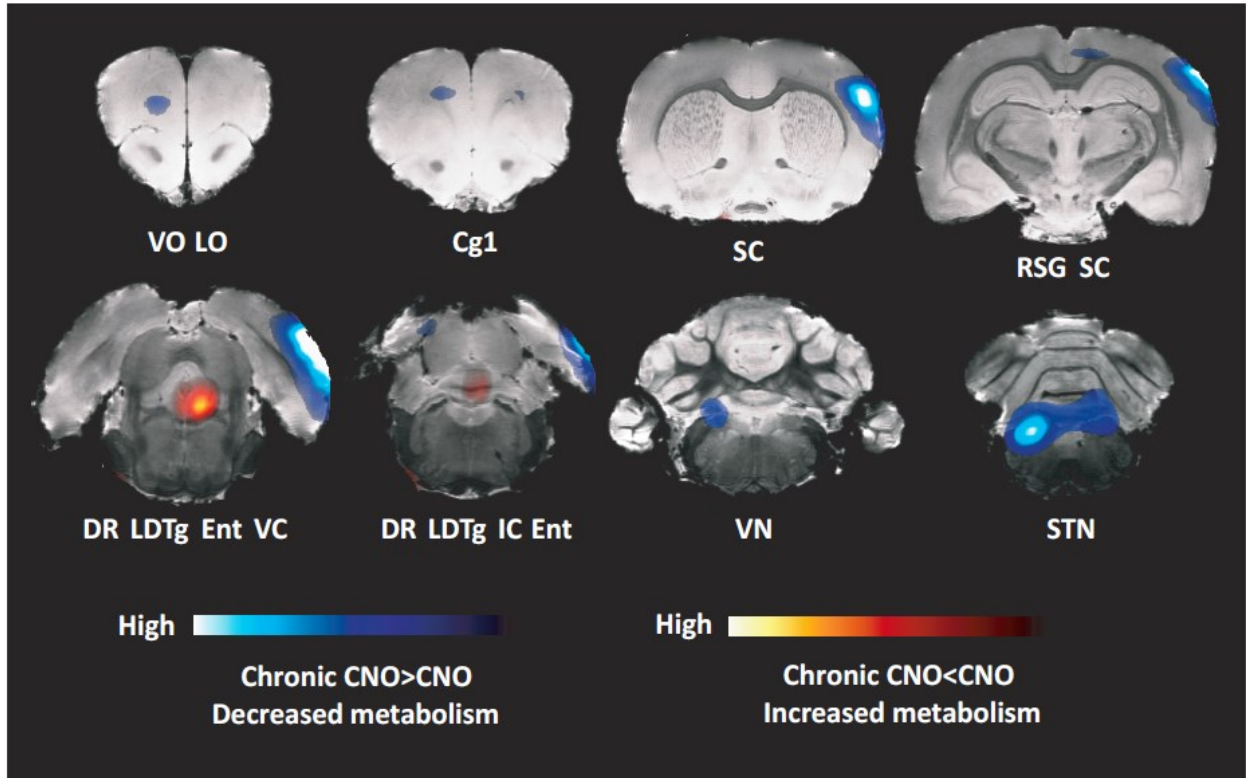
Figure 13. DREAMM responses after chronic CNO treatment followed with an acute injection of CNO

DREAMM responses after chronic CNO treatment followed with an acute injection of CNO (p=0.05, relative increase (red) and decrease (blue) in FDG uptake; N = 8, comparison of chronic CNO versus chronic CNO + Acute injection of CNO scans: within-subject comparison). Abbreviations: VO – ventral orbital cortex, LO – lateral orbital cortex, Cg1 – cingulate cortex, SC – somatosensory cortex, RSG – retrosplenial cortex, VC – visual cortex, Ent – entorhinal cortex, DR – dorsal raphe nuclei, LDTg – laterodorsal temgental nucleus, IC – inferior colliculus, VN – vestibular nuclei, and SPN – spinal trigeminal nuclei.

REFERENCES

Abbas AI, Yadav PN, Yao WD, Arbuckle MI, Grant SG, Caron MG and Roth BL (2009) PSD-95 is essential for hallucinogen and atypical antipsychotic drug actions at serotonin receptors. J Neurosci 29(22):7124-7136.

Abrams JK, Johnson PL, Hay-Schmidt A, Mikkelsen JD, Shekhar A and Lowry CA (2005) Serotonergic systems associated with arousal and vigilance behaviors following administration of anxiogenic drugs. Neuroscience 133(4):983-997.

Abrams JK, Johnson PL, Hollis JH and Lowry CA (2004) Anatomic and functional topography of the dorsal raphe nucleus. Ann N Y Acad Sci 1018:46-57.

Adell A and Artigas F (1991) Differential effects of clomipramine given locally or systemically on extracellular 5-hydroxytryptamine in raphe nuclei and frontal cortex. An in vivo brain microdialysis study. Naunyn Schmiedebergs Arch Pharmacol 343(3):237-244.

Aghajanian GK, Haigler HJ and Bloom FE (1972) Lysergic acid diethylamide and serotonin: direct actions on serotonin-containing neurons in rat brain. Life Sci I 11(13):615-622.

Alexander GM, Rogan SC, Abbas AI, Armbruster BN, Pei Y, Allen JA, Nonneman RJ, Hartmann J, Moy SS, Nicolelis MA, McNamara JO and Roth BL (2009) Remote control of neuronal activity in transgenic mice expressing evolved G protein-coupled receptors. Neuron 63(1):27-39.

Alvarez-Curto E, Prihandoko R, Tautermann CS, Zwier JM, Pediani JD, Lohse MJ, Hoffmann C, Tobin AB and Milligan G (2011) Developing chemical genetic approaches to explore G protein-coupled receptor function: validation of the use of a receptor activated solely by synthetic ligand (RASSL). Mol Pharmacol 80(6):1033-1046.

Amat J, Baratta MV, Paul E, Bland ST, Watkins LR and Maier SF (2005) Medial prefrontal cortex determines how stressor controllability affects behavior and dorsal raphe nucleus. Nat Neurosci 8(3):365-371.

Amat J, Matus-Amat P, Watkins LR and Maier SF (1998a) Escapable and inescapable stress differentially alter extracellular levels of 5-HT in the basolateral amygdala of the rat. Brain Res 812(1-2):113-120.

Amat J, Matus-Amat P, Watkins LR and Maier SF (1998b) Escapable and inescapable stress differentially and selectively alter extracellular levels of 5-HT in the ventral hippocampus and dorsal periaqueductal gray of the rat. Brain Res 797(1):12-22.

Araneda R and Andrade R (1991) 5-Hydroxytryptamine2 and 5-hydroxytryptamine 1A receptors mediate opposing responses on membrane excitability in rat association cortex. Neuroscience 40(2):399-412.

Armbruster BN, Li X, Pausch MH, Herlitze S and Roth BL (2007) Evolving the lock to fit the key to create a family of G protein-coupled receptors potently activated by an inert ligand. Proc Natl Acad Sci U S A 104(12):5163-5168.

Artaiz I, Zazpe A and Del Rio J (1998) Characterization of serotonergic mechanisms involved in the behavioural inhibition induced by 5-hydroxytryptophan in a modified light-dark test in mice. Behav Pharmacol 9(2):103-112.

Azmitia E and Gannon P (1983) The ultrastructural localization of serotonin immunoreactivity in myelinated and unmyelinated axons within the medial forebrain bundle of rat and monkey. J Neurosci 3(10):2083-2090.

Baker KG, Halliday GM, Halasz P, Hornung JP, Geffen LB, Cotton RG and Tork I (1991) Cytoarchitecture of serotonin-synthesizing neurons in the pontine tegmentum of the human brain. Synapse 7(4):301-320.

Baker KG, Halliday GM and Tork I (1990) Cytoarchitecture of the human dorsal raphe nucleus. J Comp Neurol 301(2):147-161.

Barton CL and Hutson PH (1999) Inhibition of hippocampal 5-HT synthesis by fluoxetine and paroxetine: evidence for the involvement of both 5-HT1A and 5-HT1B/D autoreceptors. Synapse 31(1):13-19.

Beaulieu JM, Zhang X, Rodriguiz RM, Sotnikova TD, Cools MJ, Wetsel WC, Gainetdinov RR and Caron MG (2008) Role of GSK3 beta in behavioral abnormalities induced by serotonin deficiency. Proc Natl Acad Sci U S A 105(4):1333-1338.

Behzadi G, Kalen P, Parvopassu F and Wiklund L (1990) Afferents to the median raphe nucleus of the rat: retrograde cholera toxin and wheat germ conjugated horseradish peroxidase tracing, and selective D-[3H]aspartate labelling of possible excitatory amino acid inputs. Neuroscience 37(1):77-100.

Berger M, Gray JA and Roth BL (2009) The expanded biology of serotonin. Annu Rev Med 60:355-366.

Binder EB and Nemeroff CB (2010) The CRF system, stress, depression and anxiety-insights from human genetic studies. Mol Psychiatry 15(6):574-588.

Blier P (2003) The pharmacology of putative early-onset antidepressant strategies. Eur Neuropsychopharmacol 13(2):57-66.

Blier P and de Montigny C (1994) Current advances and trends in the treatment of depression. Trends Pharmacol Sci 15(7):220-226.

Boyden ES, Zhang F, Bamberg E, Nagel G and Deisseroth K (2005) Millisecond-timescale, genetically targeted optical control of neural activity. Nat Neurosci 8(9):1263-1268.

Brewerton TD (1995) Toward a unified theory of serotonin dysregulation in eating and related disorders. Psychoneuroendocrinology 20(6):561-590.

Brody AL, Saxena S, Stoessel P, Gillies LA, Fairbanks LA, Alborzian S, Phelps ME, Huang SC, Wu HM, Ho ML, Ho MK, Au SC, Maidment K and Baxter LR, Jr. (2001) Regional brain metabolic changes in patients with major depression treated with either paroxetine or interpersonal therapy: preliminary findings. Arch Gen Psychiatry 58(7):631-640.

Brown M, Bing C, King P, Pickavance L, Heal D and Wilding J (2001) Sibutramine reduces feeding, body fat and improves insulin resistance in dietary-obese male Wistar rats independently of hypothalamic neuropeptide Y. Br J Pharmacol 132(8):1898-1904.

Bunin MA and Wightman RM (1998) Quantitative evaluation of 5-hydroxytryptamine (serotonin) neuronal release and uptake: an investigation of extrasynaptic transmission. J Neurosci 18(13):4854-4860.

Burghardt NS, Bush DE, McEwen BS and LeDoux JE (2007) Acute selective serotonin reuptake inhibitors increase conditioned fear expression: blockade with a 5-HT(2C) receptor antagonist. Biol Psychiatry 62(10):1111-1118.

Calizo LH, Akanwa A, Ma X, Pan YZ, Lemos JC, Craige C, Heemstra LA and Beck SG (2011) Raphe serotonin neurons are not homogenous: electrophysiological, morphological and neurochemical evidence. Neuropharmacology 61(3):524-543.

Carrasco GA and Van de Kar LD (2003) Neuroendocrine pharmacology of stress. Eur J Pharmacol 463(1-3):235-272.

Chaudhury D, Walsh JJ, Friedman AK, Juarez B, Ku SM, Koo JW, Ferguson D, Tsai HC, Pomeranz L, Christoffel DJ, Nectow AR, Ekstrand M, Domingos A, Mazei-Robison MS, Mouzon E, Lobo MK, Neve RL, Friedman JM, Russo SJ, Deisseroth K, Nestler EJ and Han MH (2013) Rapid regulation of depression-related behaviours by control of midbrain dopamine neurons. Nature 493(7433):532-536.

Cheng LL, Wang SJ and Gean PW (1998) Serotonin depresses excitatory synaptic transmission and depolarization-evoked Ca2+ influx in rat basolateral amygdala via 5-HT1A receptors. Eur J Neurosci 10(6):2163-2172.

Chua P, Krams M, Toni I, Passingham R and Dolan R (1999) A functional anatomy of anticipatory anxiety. Neuroimage 9(6 Pt 1):563-571.

Commons KG, Connolley KR and Valentino RJ (2003) A neurochemically distinct dorsal raphe-limbic circuit with a potential role in affective disorders. Neuropsychopharmacology 28(2):206-215.

Conklin BR, Hsiao EC, Claeysen S, Dumuis A, Srinivasan S, Forsayeth JR, Guettier JM, Chang WC, Pei Y, McCarthy KD, Nissenson RA, Wess J, Bockaert J and Roth BL (2008) Engineering GPCR signaling pathways with RASSLs. Nat Methods 5(8):673-678.

Crawley JN (1985) Exploratory behavior models of anxiety in mice. Neurosci Biobehav Rev 9(1):37-44.

Crick F (1999) The impact of molecular biology on neuroscience. Philos Trans R Soc Lond B Biol Sci 354(1392):2021-2025.

Crick FH (1979) Thinking about the brain. Sci Am 241(3):219-232.

Dahlstrom A and Fuxe K (1964) Localization of monoamines in the lower brain stem. Experientia 20(7):398-399.

David DJ, Samuels BA, Rainer Q, Wang JW, Marsteller D, Mendez I, Drew M, Craig DA, Guiard BP, Guilloux JP, Artymyshyn RP, Gardier AM, Gerald C, Antonijevic IA, Leonardo ED and Hen R (2009) Neurogenesis-dependent and -independent effects of fluoxetine in an animal model of anxiety/depression. Neuron 62(4):479-493.

Davidson C and Stamford JA (1995) Evidence that 5-hydroxytryptamine release in rat dorsal raphe nucleus is controlled by 5-HT1A, 5-HT1B and 5-HT1D autoreceptors. Br J Pharmacol 114(6):1107-1109.

Day HE, Greenwood BN, Hammack SE, Watkins LR, Fleshner M, Maier SF and Campeau S (2004) Differential expression of 5HT-1A, alpha 1b adrenergic, CRF-R1, and CRF-R2 receptor mRNA in serotonergic, gamma-aminobutyric acidergic, and catecholaminergic cells of the rat dorsal raphe nucleus. J Comp Neurol 474(3):364-378.

Den Boer JA and Westenberg HG (1990) Serotonin function in panic disorder: a double blind placebo controlled study with fluvoxamine and ritanserin. Psychopharmacology (Berl) 102(1):85-94.

den Boer JA, Westenberg HG, Kamerbeek WD, Verhoeven WM and Kahn RS (1987) Effect of serotonin uptake inhibitors in anxiety disorders; a double-blind comparison of clomipramine and fluvoxamine. Int Clin Psychopharmacol 2(1):21-32.

Descarries L, Riad, M. & Parent, M. (2010) Ultrastructure of the serotonin innervation in the mammalian central nervous system., in Handbook of the behavioral neurobiology of serotonin (Muller CP, Jacobs, B.L. ed) pp pp. 65-101, Amsterdam, The Netherlands:Elsevier.

Descarries L, Watkins KC, Garcia S and Beaudet A (1982) The serotonin neurons in nucleus raphe dorsalis of adult rat: a light and electron microscope radioautographic study. J Comp Neurol 207(3):239-254.

Doupnik CA, Davidson N, Lester HA and Kofuji P (1997) RGS proteins reconstitute the rapid gating kinetics of gbetagamma-activated inwardly rectifying K+ channels. Proc Natl Acad Sci U S A 94(19):10461-10466.

Farnebo LO and Hamberger B (1971) Drug-induced changes in the release of 3 H-monoamines from field stimulated rat brain slices. Acta Physiol Scand Suppl 371:35-44.

Farrell MS and Roth BL (2012) Pharmacosynthetics: Reimagining the pharmacogenetic approach. Brain Res 1511:6-20.

Fetissov SO and Meguid MM (2010) Serotonin delivery into the ventromedial nucleus of the hypothalamus affects differently feeding pattern and body weight in obese and lean Zucker rats. Appetite 54(2):346-353.

Filip M and Bader M (2009) Overview on 5-HT receptors and their role in physiology and pathology of the central nervous system. Pharmacol Rep 61(5):761-777.

Fletcher PJ and Burton MJ (1986) Dissociation of the anorectic actions of 5-HTP and fenfluramine. Psychopharmacology (Berl) 89(2):216-220.

Fletcher PJ and Paterson IA (1989) A comparison of the effects of tryptamine and 5-hydroxytryptamine on feeding following injection into the paraventricular nucleus of the hypothalamus. Pharmacol Biochem Behav 32(4):907-911.

Fu W, Le Maitre E, Fabre V, Bernard JF, David Xu ZQ and Hokfelt T (2010) Chemical neuroanatomy of the dorsal raphe nucleus and adjacent structures of the mouse brain. J Comp Neurol 518(17):3464-3494.

Gonzalez LE, Andrews N and File SE (1996) 5-HT1A and benzodiazepine receptors in the basolateral amygdala modulate anxiety in the social interaction test, but not in the elevated plus-maze. Brain Res 732(1-2):145-153.

Gorman JM, Liebowitz MR, Fyer AJ, Goetz D, Campeas RB, Fyer MR, Davies SO and Klein DF (1987) An open trial of fluoxetine in the treatment of panic attacks. J Clin Psychopharmacol 7(5):329-332.

Gothert M and Weinheimer G (1979) Extracellular 5-hydroxytryptamine inhibits 5-hydroxytryptamine release from rat brain cortex slices. Naunyn Schmiedebergs Arch Pharmacol 310(1):93-96.

Goulding EH, Schenk AK, Juneja P, MacKay AW, Wade JM and Tecott LH (2008) A robust automated system elucidates mouse home cage behavioral structure. Proc Natl Acad Sci U S A 105(52):20575-20582.

Graeff FG, Guimaraes FS, De Andrade TG and Deakin JF (1996) Role of 5-HT in stress, anxiety, and depression. Pharmacol Biochem Behav 54(1):129-141.

Graeff FG, Viana MB and Mora PO (1997) Dual role of 5-HT in defense and anxiety. Neurosci Biobehav Rev 21(6):791-799.

Grahn RE, Will MJ, Hammack SE, Maswood S, McQueen MB, Watkins LR and Maier SF (1999) Activation of serotonin-immunoreactive cells in the dorsal raphe nucleus in rats exposed to an uncontrollable stressor. Brain Res 826(1):35-43.

Gras C, Herzog E, Bellenchi GC, Bernard V, Ravassard P, Pohl M, Gasnier B, Giros B and El Mestikawy S (2002) A third vesicular glutamate transporter expressed by cholinergic and serotoninergic neurons. J Neurosci 22(13):5442-5451.

Guettier JM, Gautam D, Scarselli M, Ruiz de Azua I, Li JH, Rosemond E, Ma X, Gonzalez FJ, Armbruster BN, Lu H, Roth BL and Wess J (2009) A chemical-genetic approach to study G protein regulation of beta cell function in vivo. Proc Natl Acad Sci U S A 106(45):19197-19202.

Guler AD, Rainwater A, Parker JG, Jones GL, Argilli E, Arenkiel BR, Ehlers MD, Bonci A, Zweifel LS and Palmiter RD (2012) Transient activation of specific neurons in mice by selective expression of the capsaicin receptor. Nat Commun 3:746.

Hajos M, Richards CD, Szekely AD and Sharp T (1998) An electrophysiological and neuroanatomical study of the medial prefrontal cortical projection to the midbrain raphe nuclei in the rat. Neuroscience 87(1):95-108.

Halberstadt AL and Balaban CD (2008) Selective anterograde tracing of nonserotonergic projections from dorsal raphe nucleus to the basal forebrain and extended amygdala. J Chem Neuroanat 35(4):317-325.

Halford JC, Harrold JA, Boyland EJ, Lawton CL and Blundell JE (2007) Serotonergic drugs : effects on appetite expression and use for the treatment of obesity. Drugs 67(1):27-55.

Hasler G, Drevets WC, Manji HK and Charney DS (2004) Discovering endophenotypes for major depression. Neuropsychopharmacology 29(10):1765-1781.

Heisler LK, Cowley MA, Tecott LH, Fan W, Low MJ, Smart JL, Rubinstein M, Tatro JB, Marcus JN, Holstege H, Lee CE, Cone RD and Elmquist JK (2002) Activation of central melanocortin pathways by fenfluramine. Science 297(5581):609-611.

Heisler LK, Jobst EE, Sutton GM, Zhou L, Borok E, Thornton-Jones Z, Liu HY, Zigman JM, Balthasar N, Kishi T, Lee CE, Aschkenasi CJ, Zhang CY, Yu J, Boss O, Mountjoy KG, Clifton PG, Lowell BB, Friedman JM, Horvath T, Butler AA, Elmquist JK and Cowley MA (2006) Serotonin reciprocally regulates melanocortin neurons to modulate food intake. Neuron 51(2):239-249.

Hendricks TJ, Fyodorov DV, Wegman LJ, Lelutiu NB, Pehek EA, Yamamoto B, Silver J, Weeber EJ, Sweatt JD and Deneris ES (2003) Pet-1 ETS gene plays a critical role in 5-HT neuron development and is required for normal anxiety-like and aggressive behavior. Neuron 37(2):233-247.

Hensler JG (2002) Differential regulation of 5-HT1A receptor-G protein interactions in brain following chronic antidepressant administration. Neuropsychopharmacology 26(5):565-573.

Hioki H, Nakamura H, Ma YF, Konno M, Hayakawa T, Nakamura KC, Fujiyama F and Kaneko T (2009) Vesicular glutamate transporter 3-expressing nonserotonergic projection neurons constitute a subregion in the rat midbrain raphe nuclei. J Comp Neurol 518(5):668-686.

Hjorth S and Auerbach SB (1994) Further evidence for the importance of 5-HT1A autoreceptors in the action of selective serotonin reuptake inhibitors. Eur J Pharmacol 260(2-3):251-255.

Hoffman BJ, Hansson SR, Mezey E and Palkovits M (1998) Localization and dynamic regulation of biogenic amine transporters in the mammalian central nervous system. Front Neuroendocrinol 19(3):187-231.

Hokfelt T, Elde R, Johansson O, Terenius L and Stein L (1977) The distribution of enkephalin-immunoreactive cell bodies in the rat central nervous system. Neurosci Lett 5(1-2):25-31.

Hokfelt T, Ljungdahl A, Steinbusch H, Verhofstad A, Nilsson G, Brodin E, Pernow B and Goldstein M (1978) Immunohistochemical evidence of substance P-like immunoreactivity in some 5-hydroxytryptamine-containing neurons in the rat central nervous system. Neuroscience 3(6):517-538.

Hornung JP (2003) The human raphe nuclei and the serotonergic system. J Chem Neuroanat 26(4):331-343.

Hornung JP (2010) The Neuronatomy of the Serotonergic System, in Handbook of the behavioral neurobiology of serotonin (Muller CP, Jacobs, B.L. ed) pp pp. 51-64, Amsterdam, The Netherlands:Elsevier.

Jacobs BL and Azmitia EC (1992) Structure and function of the brain serotonin system. Physiol Rev 72(1):165-229.

Jacobsen JP, Siesser WB, Sachs BD, Peterson S, Cools MJ, Setola V, Folgering JH, Flik G and Caron MG (2012) Deficient serotonin neurotransmission and depression-like serotonin biomarker alterations in tryptophan hydroxylase 2 (Tph2) loss-of-function mice. Mol Psychiatry 17(7):694-704.

Javanmard M, Shlik J, Kennedy SH, Vaccarino FJ, Houle S and Bradwejn J (1999) Neuroanatomic correlates of CCK-4-induced panic attacks in healthy humans: a comparison of two time points. Biol Psychiatry 45(7):872-882.

Jennes L, Stumpf WE and Kalivas PW (1982) Neurotensin: topographical distribution in rat brain by immunohistochemistry. J Comp Neurol 210(3):211-224.

Jensen P, Farago AF, Awatramani RB, Scott MM, Deneris ES and Dymecki SM (2008) Redefining the serotonergic system by genetic lineage. Nat Neurosci 11(4):417-419

.

Jimerson DC, Lesem MD, Kaye WH, Hegg AP and Brewerton TD (1990) Eating disorders and depression: is there a serotonin connection? Biol Psychiatry 28(5):443-454.

Kaufmann A, Keim A and Thiel G (2013) Regulation of immediate-early gene transcription following activation of Galpha(q)-coupled designer receptors. J Cell Biochem 114(3):681-696.

Kennedy SH, Evans KR, Kruger S, Mayberg HS, Meyer JH, McCann S, Arifuzzman AI, Houle S and Vaccarino FJ (2001) Changes in regional brain glucose metabolism measured with positron emission tomography after paroxetine treatment of major depression. Am J Psychiatry 158(6):899-905.

Kirby LG, Allen AR and Lucki I (1995) Regional differences in the effects of forced swimming on extracellular levels of 5-hydroxytryptamine and 5-hydroxyindoleacetic acid. Brain Res 682(1-2):189-196.

Kosofsky BE and Molliver ME (1987) The serotoninergic innervation of cerebral cortex: different classes of axon terminals arise from dorsal and median raphe nuclei. Synapse 1(2):153-168.

Koyama S, Matsumoto N, Murakami N, Kubo C, Nabekura J and Akaike N (2002) Role of presynaptic 5-HT1A and 5-HT3 receptors in modulation of synaptic GABA transmission in dissociated rat basolateral amygdala neurons. Life Sci 72(4-5):375-387.

Krashes MJ, Koda S, Ye C, Rogan SC, Adams AC, Cusher DS, Maratos-Flier E, Roth BL and Lowell BB (2011) Rapid, reversible activation of AgRP neurons drives feeding behavior in mice. J Clin Invest 121(4):1424-1428.

Kreiss DS and Lucki I (1995) Effects of acute and repeated administration of antidepressant drugs on extracellular levels of 5-hydroxytryptamine measured in vivo. J Pharmacol Exp Ther 274(2):866-876.

Krishnan V and Nestler EJ (2008) The molecular neurobiology of depression. Nature 455(7215):894-902.

Kroenke K, West SL, Swindle R, Gilsenan A, Eckert GJ, Dolor R, Stang P, Zhou XH, Hays R and Weinberger M (2001) Similar effectiveness of paroxetine, fluoxetine, and sertraline in primary care: a randomized trial. JAMA 286(23):2947-2955.

Kroeze WK and Roth BL (1998) The molecular biology of serotonin receptors: therapeutic implications for the interface of mood and psychosis. Biol Psychiatry 44(11):1128-1142.

Leibowitz SF and Alexander JT (1998) Hypothalamic serotonin in control of eating behavior, meal size, and body weight. Biol Psychiatry 44(9):851-864.

Lerer B, Gelfin Y, Gorfine M, Allolio B, Lesch KP and Newman ME (1999) 5-HT1A receptor function in normal subjects on clinical doses of fluoxetine: blunted temperature and hormone responses to ipsapirone challenge. Neuropsychopharmacology 20(6):628-639.

Levy AD and Van de Kar LD (1992) Endocrine and receptor pharmacology of serotonergic anxiolytics, antipsychotics and antidepressants. Life Sci 51(2):83-94.

Li B, Piriz J, Mirrione M, Chung C, Proulx CD, Schulz D, Henn F and Malinow R (2011) Synaptic potentiation onto habenula neurons in the learned helplessness model of depression. Nature 470(7335):535-539.

Li Q, Muma NA and van de Kar LD (1996) Chronic fluoxetine induces a gradual desensitization of 5-HT1A receptors: reductions in hypothalamic and midbrain Gi and G(o) proteins and in neuroendocrine responses to a 5-HT1A agonist. J Pharmacol Exp Ther 279(2):1035-1042.

Li YQ, Jia HG, Rao ZR and Shi JW (1990) Serotonin-, substance P- or leucine-enkephalin-containing neurons in the midbrain periaqueductal gray and nucleus raphe dorsalis send projection fibers to the central amygdaloid nucleus in the rat. Neurosci Lett 120(1):124-127.

Lidov HG and Molliver ME (1982) Immunohistochemical study of the development of serotonergic neurons in the rat CNS. Brain Res Bull 9(1-6):559-604.

Lowry CA (2002) Functional subsets of serotonergic neurones: implications for control of the hypothalamic-pituitary-adrenal axis. J Neuroendocrinol 14(11):911-923.

Lowry CA, Hale MW, Evans AK, Heerkens J, Staub DR, Gasser PJ and Shekhar A (2008) Serotonergic systems, anxiety, and affective disorder: focus on the dorsomedial part of the dorsal raphe nucleus. Ann N Y Acad Sci 1148:86-94.

Lucas JJ, Yamamoto A, Scearce-Levie K, Saudou F and Hen R (1998) Absence of fenfluramine-induced anorexia and reduced c-Fos induction in the hypothalamus and central amygdaloid complex of serotonin 1B receptor knock-out mice. J Neurosci 18(14):5537-5544.

Lucki I (1998) The spectrum of behaviors influenced by serotonin. Biol Psychiatry 44(3):151-162.

Luyten L, Casteels C, Vansteenwegen D, van Kuyck K, Koole M, Van Laere K and Nuttin B (2012) Micro-positron emission tomography imaging of rat brain metabolism during expression of contextual conditioning. J Neurosci 32(1):254-263.

Maes M, Meltzer HY (1995) The serotonin hypothesis of major depression., in Psychopharmacology: The Fourth Generation of Progress (Bloom FE, Kupfer DJ ed) pp pp. 933-944, Raven Press, New York.

Matthews PR and Harrison PJ (2012) A morphometric, immunohistochemical, and in situ hybridization study of the dorsal raphe nucleus in major depression, bipolar disorder, schizophrenia, and suicide. J Affect Disord 137(1-3):125-134.

Mayberg HS, Brannan SK, Tekell JL, Silva JA, Mahurin RK, McGinnis S and Jerabek PA (2000) Regional metabolic effects of fluoxetine in major depression: serial changes and relationship to clinical response. Biol Psychiatry 48(8):830-843.

McDevitt RA and Neumaier JF (2012) Regulation of dorsal raphe nucleus function by serotonin autoreceptors: a behavioral perspective. J Chem Neuroanat 41(4):234-246.

Michaelides M, Anderson SA, Ananth M, Smirnov D, Thanos PK, Neumaier JF, Wang GJ, Volkow ND and Hurd YL (2013) In vivo cell-specific mesocorticolimbic whole-brain circuit dissection in freely-moving animals. J Clin Invest In press.

Michaelides M, Pascau J, Gispert JD, Delis F, Grandy DK, Wang GJ, Desco M, Rubinstein M, Volkow ND and Thanos PK (2010) Dopamine D4 receptors modulate brain metabolic activity in the prefrontal cortex and cerebellum at rest and in response to methylphenidate. Eur J Neurosci 32(4):668-676.

Middlemiss DN and Hutson PH (1990) The 5-HT1B receptors. Ann N Y Acad Sci 600:132-147; discussion 347-148.

Moret C and Briley M (1996) Effects of acute and repeated administration of citalopram on extracellular levels of serotonin in rat brain. Eur J Pharmacol 295(2-3):189-197.

Muller JF, Mascagni F and McDonald AJ (2007) Serotonin-immunoreactive axon terminals innervate pyramidal cells and interneurons in the rat basolateral amygdala. J Comp Neurol 505(3):314-335.

Nawaratne V, Leach K, Suratman N, Loiacono RE, Felder CC, Armbruster BN, Roth BL, Sexton PM and Christopoulos A (2008) New insights into the function of M4 muscarinic acetylcholine receptors gained using a novel allosteric modulator and a DREADD (designer receptor exclusively activated by a designer drug). Mol Pharmacol 74(4):1119-1131.

Nestler EJ, Barrot M, DiLeone RJ, Eisch AJ, Gold SJ and Monteggia LM (2002) Neurobiology of depression. Neuron 34(1):13-25.

Nierenberg AA, Farabaugh AH, Alpert JE, Gordon J, Worthington JJ, Rosenbaum JF and Fava M (2000) Timing of onset of antidepressant response with fluoxetine treatment. Am J Psychiatry 157(9):1423-1428.

Nurnberg HG, Thompson PM and Hensley PL (1999) Antidepressant medication change in a clinical treatment setting: a comparison of the effectiveness of selective serotonin reuptake inhibitors. J Clin Psychiatry 60(9):574-579.

Ochi J and Shimizu K (1978) Occurrence of dopamine-containing neurons in the midbrain raphe nuclei of the rat. Neurosci Lett 8(4):317-320.

Penington NJ, Kelly JS and Fox AP (1993) Whole-cell recordings of inwardly rectifying K+ currents activated by 5-HT1A receptors on dorsal raphe neurones of the adult rat. J Physiol 469:387-405.

Peters JA, Malone HM and Lambert JJ (1992) Recent advances in the electrophysiological characterization of 5-HT3 receptors. Trends Pharmacol Sci 13(10):391-397.

Peyron C, Petit JM, Rampon C, Jouvet M and Luppi PH (1998) Forebrain afferents to the rat dorsal raphe nucleus demonstrated by retrograde and anterograde tracing methods. Neuroscience 82(2):443-468.

Pineyro G and Blier P (1996) Regulation of 5-hydroxytryptamine release from rat midbrain raphe nuclei by 5-hydroxytryptamine1D receptors: effect of tetrodotoxin, G protein inactivation and long-term antidepressant administration. J Pharmacol Exp Ther 276(2):697-707.

Pogorelov VM, Rodriguiz RM, Insco ML, Caron MG and Wetsel WC (2005) Novelty seeking and stereotypic activation of behavior in mice with disruption of the Dat1 gene. Neuropsychopharmacology 30(10):1818-1831.

Porsolt RD, Le Pichon M and Jalfre M (1977) Depression: a new animal model sensitive to antidepressant treatments. Nature 266(5604):730-732.

Raap DK, Evans S, Garcia F, Li Q, Muma NA, Wolf WA, Battaglia G and Van De Kar LD (1999) Daily injections of fluoxetine induce dose-dependent desensitization of hypothalamic 5-HT1A receptors: reductions in neuroendocrine responses to 8-OH-DPAT and in levels of Gz and Gi proteins. J Pharmacol Exp Ther 288(1):98-106.

Rapport MM, Green AA and Page IH (1948) Crystalline Serotonin. Science 108(2804):329-330.

Ray RS, Corcoran AE, Brust RD, Kim JC, Richerson GB, Nattie E and Dymecki SM (2011) Impaired respiratory and body temperature control upon acute serotonergic neuron inhibition. Science 333(6042):637-642.

Rees S, den Daas I, Foord S, Goodson S, Bull D, Kilpatrick G and Lee M (1994) Cloning and characterisation of the human 5-HT5A serotonin receptor. FEBS Lett 355(3):242-246.
Rogan SC and Roth BL (2011) Remote control of neuronal signaling. Pharmacol Rev 63(2):291-315.

Roiser JP, Levy J, Fromm SJ, Nugent AC, Talagala SL, Hasler G, Henn FA, Sahakian BJ and Drevets WC (2009) The effects of tryptophan depletion on neural responses to emotional words in remitted depression. Biol Psychiatry 66(5):441-450.

Roth BL (2006) The serotonin receptors : from molecular pharmacology to human therapeutics. Humana Press, Totowa, N.J.

Rothman RB, Baumann MH, Savage JE, Rauser L, McBride A, Hufeisen SJ and Roth BL (2000) Evidence for possible involvement of 5-HT(2B) receptors in the cardiac valvulopathy associated with fenfluramine and other serotonergic medications. Circulation 102(23):2836-2841.

Rueter LE, Fornal CA and Jacobs BL (1997) A critical review of 5-HT brain microdialysis and behavior. Rev Neurosci 8(2):117-137.

Salegio EA, Samaranch L, Kells AP, Mittermeyer G, San Sebastian W, Zhou S, Beyer J, Forsayeth J and Bankiewicz KS (2013) Axonal transport of adeno-associated viral vectors is serotype-dependent. Gene Ther 20(3):348-352.

Saller CF and Stricker EM (1976) Hyperphagia and increased growth in rats after intraventricular injection of 5,7-dihydroxytryptamine. Science 192(4237):385-387.

Santarelli L, Saxe M, Gross C, Surget A, Battaglia F, Dulawa S, Weisstaub N, Lee J, Duman R, Arancio O, Belzung C and Hen R (2003) Requirement of hippocampal neurogenesis for the behavioral effects of antidepressants. Science 301(5634):805-809.

Sartorius A, Kiening KL, Kirsch P, von Gall CC, Haberkorn U, Unterberg AW, Henn FA and Meyer-Lindenberg A (2010) Remission of major depression under deep brain stimulation of the lateral habenula in a therapy-refractory patient. Biol Psychiatry 67(2):e9-e11.

Seminowicz DA, Mayberg HS, McIntosh AR, Goldapple K, Kennedy S, Segal Z and Rafi-Tari S (2004) Limbic-frontal circuitry in major depression: a path modeling metanalysis. Neuroimage 22(1):409-418.

Shabel SJ, Proulx CD, Trias A, Murphy RT and Malinow R (2012) Input to the lateral habenula from the basal ganglia is excitatory, aversive, and suppressed by serotonin. Neuron 74(3):475-481.

Shaw DM, Camps FE and Eccleston EG (1967) 5-Hydroxytryptamine in the hind-brain of depressive suicides. Br J Psychiatry 113(505):1407-1411.

Shopsin B, Friedman E and Gershon S (1976) Parachlorophenylalanine reversal of tranylcypromine effects in depressed patients. Arch Gen Psychiatry 33(7):811-819.

Shopsin B, Gershon S, Goldstein M, Friedman E and Wilk S (1975) Use of synthesis inhibitors in defining a role for biogenic amines during imipramine treatment in depressed patients. Psychopharmacol Commun 1(2):239-249.

Shumake J, Colorado RA, Barrett DW and Gonzalez-Lima F (2010) Metabolic mapping of the effects of the antidepressant fluoxetine on the brains of congenitally helpless rats. Brain Res 1343:218-225.

Singewald N and Sharp T (2000) Neuroanatomical targets of anxiogenic drugs in the hindbrain as revealed by Fos immunocytochemistry. Neuroscience 98(4):759-770.

Stahl SM (2008) Stahl's essential psychopharmacology neuroscientific basis and practical applications, pp 1 online resource (xv, 1117 p.), Cambridge University Press, Cambridge ; New York.

Stamford JA, Davidson C, McLaughlin DP and Hopwood SE (2000) Control of dorsal raphe 5-HT function by multiple 5-HT(1) autoreceptors: parallel purposes or pointless plurality? Trends Neurosci 23(10):459-465.

Staub DR, Evans AK and Lowry CA (2006) Evidence supporting a role for corticotropin-releasing factor type 2 (CRF2) receptors in the regulation of subpopulations of serotonergic neurons. Brain Res 1070(1):77-89.

Staub DR, Spiga F and Lowry CA (2005) Urocortin 2 increases c-Fos expression in topographically organized subpopulations of serotonergic neurons in the rat dorsal raphe nucleus. Brain Res 1044(2):176-189.

Steinbusch HW (1981) Distribution of serotonin-immunoreactivity in the central nervous system of the rat-cell bodies and terminals. Neuroscience 6(4):557-618.

Steinbusch HW, Nieuwenhuys R, Verhofstad AA and Van der Kooy D (1981) The nucleus raphe dorsalis of the rat and its projection upon the caudatoputamen. A combined

cytoarchitectonic, immunohistochemical and retrograde transport study. J Physiol (Paris) 77(2-3):157-174.

Straube T, Schmidt S, Weiss T, Mentzel HJ and Miltner WH (2009) Dynamic activation of the anterior cingulate cortex during anticipatory anxiety. Neuroimage 44(3):975-981.

Sung KK, Jang DP, Lee S, Kim M, Lee SY, Kim YB, Park CW and Cho ZH (2009) Neural responses in rat brain during acute immobilization stress: a [F-18]FDG micro PET imaging study. Neuroimage 44(3):1074-1080.

Tecott LH (2007) Serotonin and the orchestration of energy balance. Cell Metab 6(5):352-361.

Tecott LH, Sun LM, Akana SF, Strack AM, Lowenstein DH, Dallman MF and Julius D (1995) Eating disorder and epilepsy in mice lacking 5-HT2c serotonin receptors. Nature 374(6522):542-546.

To CT, Anheuer ZE and Bagdy G (1999) Effects of acute and chronic fluoxetine treatment of CRH-induced anxiety. Neuroreport 10(3):553-555.

To CT and Bagdy G (1999) Anxiogenic effect of central CCK administration is attenuated by chronic fluoxetine or ipsapirone treatment. Neuropharmacology 38(2):279-282.

Torres GE and Amara SG (2007) Glutamate and monoamine transporters: new visions of form and function. Curr Opin Neurobiol 17(3):304-312.

Underwood MD, Khaibulina AA, Ellis SP, Moran A, Rice PM, Mann JJ and Arango V (1999) Morphometry of the dorsal raphe nucleus serotonergic neurons in suicide victims. Biol Psychiatry 46(4):473-483.

Valentino RJ, Liouterman L and Van Bockstaele EJ (2001) Evidence for regional heterogeneity in corticotropin-releasing factor interactions in the dorsal raphe nucleus. J Comp Neurol 435(4):450-463.

Vertes RP (1991) A PHA-L analysis of ascending projections of the dorsal raphe nucleus in the rat. J Comp Neurol 313(4):643-668.

Vianna DM, Graeff FG, Brandao ML and Landeira-Fernandez J (2001) Defensive freezing evoked by electrical stimulation of the periaqueductal gray: comparison between dorsolateral and ventrolateral regions. Neuroreport 12(18):4109-4112.

Vickers SP, Clifton PG, Dourish CT and Tecott LH (1999) Reduced satiating effect of d-fenfluramine in serotonin 5-HT(2C) receptor mutant mice. Psychopharmacology (Berl) 143(3):309-314.

Walther DJ, Peter JU, Bashammakh S, Hortnagl H, Voits M, Fink H and Bader M (2003) Synthesis of serotonin by a second tryptophan hydroxylase isoform. Science 299(5603):76.

Wang QP, Ochiai H and Nakai Y (1992) GABAergic innervation of serotonergic neurons in the dorsal raphe nucleus of the rat studied by electron microscopy double immunostaining. Brain Res Bull 29(6):943-948.

Wang RY and Aghajanian GK (1977) Antidromically identified serotonergic neurons in the rat midbrain raphe: evidence for collateral inhibition. Brain Res 132(1):186-193.

Warden MR, Selimbeyoglu A, Mirzabekov JJ, Lo M, Thompson KR, Kim SY, Adhikari A, Tye KM, Frank LM and Deisseroth K (2012) A prefrontal cortex-brainstem neuronal projection that controls response to behavioural challenge. Nature 492(7429):428-432.

Waselus M, Valentino RJ and Van Bockstaele EJ (2012) Collateralized dorsal raphe nucleus projections: a mechanism for the integration of diverse functions during stress. J Chem Neuroanat 41(4):266-280.

Weiner DM, Meltzer HY, Veinbergs I, Donohue EM, Spalding TA, Smith TT, Mohell N, Harvey SC, Lameh J, Nash N, Vanover KE, Olsson R, Jayathilake K, Lee M, Levey AI, Hacksell U, Burstein ES, Davis RE and Brann MR (2004) The role of M1 muscarinic receptor agonism of N-desmethylclozapine in the unique clinical effects of clozapine. Psychopharmacology (Berl) 177(1-2):207-216.

Wess J, Nakajima K and Jain S (2013) Novel designer receptors to probe GPCR signaling and physiology. Trends Pharmacol Sci 34(7):385-392.

Willner P (1990) Animal models of depression: an overview. Pharmacol Ther 45(3):425-455.

Willoughby JO and Blessing WW (1987) Origin of serotonin innervation of the arcuate and ventromedial hypothalamic region. Brain Res 418(1):170-173.

Wong KP, Sha W, Zhang X and Huang SC (2011) Effects of administration route, dietary condition, and blood glucose level on kinetics and uptake of 18F-FDG in mice. J Nucl Med 52(5):800-807.

Yen TT, Wong, DT, Bemis, KG (1987) Reduction of food consumption and body weight of normal and obese mice by chronic treatment with fluoxetine: A serotonin reuptake inhibitor. Drug Dev Res 10(1):37-45.

Young SN, Smith SE, Pihl RO and Ervin FR (1985) Tryptophan depletion causes a rapid lowering of mood in normal males. Psychopharmacology (Berl) 87(2):173-177.

Zanoveli JM, Nogueira RL and Zangrossi H, Jr. (2003) Serotonin in the dorsal periaqueductal gray modulates inhibitory avoidance and one-way escape behaviors in the elevated T-maze. Eur J Pharmacol 473(2-3):153-161.

Zhang X, Gainetdinov RR, Beaulieu JM, Sotnikova TD, Burch LH, Williams RB, Schwartz DA, Krishnan KR and Caron MG (2005) Loss-of-function mutation in tryptophan hydroxylase-2 identified in unipolar major depression. Neuron 45(1):11-16.

Zhang Y, Raap DK, Garcia F, Serres F, Ma Q, Battaglia G and Van de Kar LD (2000) Long-term fluoxetine produces behavioral anxiolytic effects without inhibiting neuroendocrine responses to conditioned stress in rats. Brain Res 855(1):58-66.